

Executive Summary of the Thesis

Synthesis and Characterization of LaX (X = O, S, F) Compounds and their Application in the field of Photoluminescence and Upconversion materials

A Thesis
Submitted to

The Maharaja Sayajirao University of Baroda
For the Award of the Degree of

Doctor of Philosophy
In

Applied Physics

By

Mr. Kevil Shah

Supervisor

Dr. Bishwajit S. Chakrabarty

Associate Professor

Department of Applied Physics

Faculty of Technology and Engineering

The M.S. University of Baroda

Vadodara-390001



Department of Applied Physics
Faculty of Technology & Engineering
The M.S. University of Baroda Vadodara
August 2021

Index

List of Figures

List of Tables

I
VI

Chapter 1:	Luminescence Properties of Rare Earth Elements	
1.1	Luminescence	2
1.2	Photoluminescence	3
1.3	Upconversion Photoluminescence: mechanism and application	5
1.4	Photoluminescence Properties of Rare Earth Elements	8
	References	13
Chapter 2:	Synthesis & Characterization of Rare Earth Doped La₂O₃: Investigation of Optical, Down conversion and Upconversion Properties	
	Abstract	16
	Graphical abstract	17
2.1	Introduction	19
2.2	Experimental Procedure	20
2.3	Results and Analysis of downconversion Samples	
	2.3.1 Structural, Morphological and Elemental analysis	22
	2.3.2 UV–Visible analysis	30
	2.3.3 Photoluminescence analysis	33
2.4	Results and Analysis of Upconversion Samples	
	2.4.1 Structural analysis	37
	2.4.2 Upconversion Photoluminescence analysis	38
2.5	Conclusion	43
	References	43
Chapter3:	UV emission and Energy transfer process in xCe³⁺, yGd³⁺: La_{2-(x+y)}O₃ & xPr³⁺, yGd³⁺: La_{2-(x+y)}O₃ Phosphors	
	Abstract	50
	Graphical abstract	51
3.1	Introduction	53
3.2	Experimental Procedure	56
3.3	Results and analysis	
	3.3.1 Structural and elemental analysis	56
	3.3.2 UV–Visible analysis	61
	3.3.3 Photoluminescence analysis	65
3.4	Conclusion	80
	References	80

**Chapter 4: Synthesis & Characterization of Rare Earth Doped La₂O₂S:
Investigation of Optical, Down conversion and Upconversion
Properties**

Abstract	86
Graphical abstract	87
4.1 Introduction	91
4.2 Experimental Procedure	
4.3 Results and Analysis of downconversion Samples	
4.3.1 Structural, Morphological and Elemental analysis	93
4.3.2 UV–Visible analysis	100
4.3.3 Photoluminescence analysis	104
4.4 Results and Analysis of Upconversion Samples	
4.4.1 Structural analysis	108
4.4.2 Upconversion Photoluminescence analysis	109
4.5 Conclusion	114
References	114

**Chapter 5: Synthesis & Characterization of Rare Earth Doped LaOF:
Investigation of Optical, Down conversion and Upconversion
Properties**

Abstract	122
Graphical abstract	123
5.1 Introduction	124
5.2 Experimental Procedure	125
5.3 Results and Analysis of downconversion Samples	
5.3.1 Structural, Morphological and Elemental analysis	128
5.3.2 UV–Visible analysis	135
5.3.3 Photoluminescence analysis	138
5.4 Results and Analysis of Upconversion Samples	
5.4.1 Structural analysis	143
5.4.2 Upconversion Photoluminescence analysis	144
5.5 Conclusion	150
References	150

List of Publications 154

Seminar/Workshop/Conference attended 155

List of Figures

Figure 1.1 One form of a Jabłoński diagram

Figure 2.1 XRD of pristine and doped La₂O₃

Figure 2.2 (a) EDAX Spectrum with mapping of La₂O₃

Figure 2.2 (b) EDAX Spectrum with mapping of 1% Pr³⁺: La₂O₃

Figure 2.2 (c) EDAX Spectrum with mapping of 1% Eu³⁺:La₂O₃

Figure 2.2 (d) EDAX Spectrum with mapping of 1% Tb³⁺: La₂O₃

Figure 2.2 (e) EDAX Spectrum with mapping of 1% Dy³⁺: La₂O₃

Figure 2.3 (a) SEM image of La₂O₃ with histogram showing particle size distribution

Figure 2.3 (b) SEM image of 1%Pr³⁺: La₂O₃ with histogram showing particle size distribution

Figure 2.3 (c) SEM image of 1%Eu³⁺: La₂O₃ with histogram showing particle size distribution

Figure 2.3 (d) SEM image of 1%Tb³⁺: La₂O₃ with histogram showing particle size distribution

Figure 2.3 (e) SEM image of 1%Dy³⁺: La₂O₃ with histogram showing particle size distribution

Figure 2.4 UV-Visible graph of 1% Ln³⁺: La₂O₃

Figure 2.5 Tauc plot Ln³⁺: La₂O₃

Figure 2.6 (a) Excitation & Emission characteristics of 1%Pr³⁺: La₂O₃

Figure 2.6 (b) Excitation & Emission characteristics of 1%Eu³⁺: La₂O₃

Figure 2.6 (c) Excitation & Emission characteristics of 1%Tb³⁺: La₂O₃

Figure 2.6 (d) Excitation & Emission characteristics of 1% Dy^{3+} : La_2O_3

Figure 2.7 Energy level diagrams for down conversion photoluminescence

Figure 2.8 XRD of upconversion samples

Figure 2.9 (a) Excitation & Emission characteristics of 12% Yb^{3+} -2% Er : La_2O_3

Figure 2.9 (b) Excitation & Emission characteristics of 12% Yb^{3+} -2% Ho : La_2O_3

Figure 2.9 (c) Excitation & Emission characteristics of 12% Yb^{3+} -2% Tm : La_2O_3

Figure 2.10 (a) Energy level diagram for Upconversion photoluminescence of 12% Yb^{3+} -2% Er^{3+} : La_2O_3

Figure 2.10 (b) Energy level diagram for Upconversion photoluminescence of 12% Yb^{3+} -2% Ho^{3+} : La_2O_3

Figure 2.10 (c) Energy level diagram for Upconversion photoluminescence of 12% Yb^{3+} -2% Tm^{3+} : La_2O_3

Figure 3.1 XRD Spectra of Synthesized Samples

Figure 3.2 EDAX Spectra of Synthesized Samples (a) 1% Ce^{3+} : La_2O_3 (b) 1% Gd^{3+} : La_2O_3 (c) 1% Ce^{3+} , 1% Gd^{3+} : La_2O_3 (d) 2% Ce^{3+} , 1% Gd^{3+} : La_2O_3 (e) 1% Pr^{3+} : La_2O_3 (f) 1% Pr^{3+} , 1% Gd^{3+} : La_2O_3 (g) 2% Pr^{3+} , 1% Gd^{3+} : La_2O_3

Figure 3.3 UV – Visible Spectra of Synthesized Samples (a) 1% Ce^{3+} : La_2O_3 (b) 1% Gd^{3+} : La_2O_3 (c) 1% Ce^{3+} , 1% Gd^{3+} : La_2O_3 (d) 2% Ce^{3+} , 1% Gd^{3+} : La_2O_3 (e) 1% Pr^{3+} : La_2O_3 (f) 1% Pr^{3+} , 1% Gd^{3+} : La_2O_3 (g) 2% Pr^{3+} , 1% Gd^{3+} : La_2O_3

Figure 3.4 Tauc's Plot of Synthesized Samples from UV – Visible Spectra

Figure 3.5 PL Excitation & Emission Spectra of Synthesized Samples (a) 1% Ce^{3+} : La_2O_3 (b) 1% Gd^{3+} : La_2O_3 (c) 1% Ce^{3+} , 1% Gd^{3+} : La_2O_3 (d) 2% Ce^{3+} , 1% Gd^{3+} : La_2O_3 (e) 1% Pr^{3+} : La_2O_3 (f) 1% Pr^{3+} , 1% Gd^{3+} : La_2O_3 (g) 2% Pr^{3+} , 1% Gd^{3+} : La_2O_3

Figure 3.6 (a) Energy transfer process diagrams for PL of rare earth ions in 1% Ce^{3+} : La_2O_3 ,

Figure 3.6 (b) Energy transfer process diagrams for PL of rare earth ions in Ce^{3+} - Gd^{3+} : La_2O_3

Figure 3.6 (c) Energy transfer process diagrams for PL of rare earth ions in Pr^{3+} - Gd^{3+} : La_2O_3

Figure 4.1 (a) XRD pattern of material synthesized by the solid-state method without flux
(b) XRD pattern for a solid-state method with flux (c) XRD pattern of a hydrothermal method without flux (d) XRD pattern for a hydrothermal method with flux (e) XRD pattern for the combustion method without flux (f) XRD pattern for the combustion method with flux

Figure 4.2 XRD pattern of pristine $\text{La}_2\text{O}_2\text{S}$ and 1% Ln^{3+} : $\text{La}_2\text{O}_2\text{S}$

Figure 4.3 (a) EDAX spectrum of 1% Pr^{3+} : $\text{La}_2\text{O}_2\text{S}$

Figure 4.3 (b) EDAX spectrum of 1% Eu^{3+} : $\text{La}_2\text{O}_2\text{S}$

Figure 4.3 (c) EDAX spectrum of 1% Tb^{3+} : $\text{La}_2\text{O}_2\text{S}$

Figure 4.3 (d) EDAX spectrum of 1% Dy^{3+} : $\text{La}_2\text{O}_2\text{S}$

Figure 4.4 UV-Visible and Tauc's Plot of pristine $\text{La}_2\text{O}_2\text{S}$

Figure 4.5 UV-Visible and Tauc's Plot of pristine $\text{La}_2\text{O}_2\text{S}$

Figure 4.6 Tauc's plot of Ln^{3+} : $\text{La}_2\text{O}_2\text{S}$

Figure 4.7(a) emission and excitation graph of doped 1% Pr^{3+} : $\text{La}_2\text{O}_2\text{S}$

Figure 4.7(b) emission and excitation graph of doped 1% Eu^{3+} : $\text{La}_2\text{O}_2\text{S}$

Figure 4.7(c) emission and excitation graph of doped 1% Tb^{3+} : $\text{La}_2\text{O}_2\text{S}$

Figure 4.7(d) emission and excitation graph of doped 1% Dy^{3+} : $\text{La}_2\text{O}_2\text{S}$

Figure 4.8 XRD of upconversion samples

Figure 4.9 (a) Excitation & Emission characteristics of 12% Yb³⁺-2% Er: La₂O₂S

Figure 4.9 (b) Excitation & Emission characteristics of 12% Yb³⁺-2% Ho: La₂O₂S

Figure 4.9 (c) Excitation & Emission characteristics of 12% Yb³⁺-2% Tm: La₂O₃

Figure 4.10 (a) Energy level diagram for Upconversion photoluminescence of 12% Yb³⁺- 2% Er³⁺: La₂O₂S

Figure 4.10 (b) Energy level diagram for Upconversion photoluminescence of 12% Yb³⁺- 2% Ho³⁺: La₂O₂S & 12% Yb³⁺- 2% Tm³⁺: La₂O₂S

Figure 5.1 XRD of pristine and doped LaOF

Figure 5.2 (a) EDAX Spectrum with mapping of LaOF

Figure 5.2 (b) EDAX Spectrum with mapping of 1% Pr³⁺: LaOF

Figure 5.2 (c) EDAX Spectrum with mapping of 1% Eu³⁺: LaOF

Figure 5.2 (d) EDAX Spectrum with mapping of 1% Tb³⁺: LaOF

Figure 5.2 (e) EDAX Spectrum with mapping of 1% Dy³⁺: LaOF

Figure 5.3 (a) SEM images with histogram of LaOF

Figure 5.3 (b) SEM images with histogram of 1% Pr³⁺: LaOF

Figure 5.3 (c) SEM images with histogram of 1% Eu³⁺: LaOF

Figure 5.3 (d) SEM images with histogram of 1% Tb³⁺: LaOF

Figure 5.3 (e) SEM images with histogram of 1% Dy³⁺: LaOF

Figure 5.4 UV-Visible characteristics of 1% Ln³⁺: LaOF

Figure 5.5 Tauc's plot for samples

Figure 5.6 (a) Excitation and Emission spectra of 1%Pr³⁺: LaOF

Figure 5.6 (b) Excitation and Emission spectra of 1%Eu³⁺: LaOF

Figure 5.6 (c) Excitation and Emission spectra of 1%Tb³⁺: LaOF

Figure 5.6 (d) Excitation and Emission spectra of 1% Dy^{3+} : LaOF

Figure 5.7 Energy level diagram for down conversion photoluminescence

Figure 5.8 XRD of upconversion samples

Figure 5.9 (a) Emission characteristics of 12% Yb^{3+} -2% Er^{3+} : LaOF

Figure 5.9 (b) Emission characteristics of 12% Yb^{3+} -2% Ho^{3+} : LaOF

Figure 5.9 (c) Emission characteristics of 12% Yb^{3+} -2% Tm^{3+} : LaOF

Figure 5.10 (a) Energy level diagram for Upconversion photoluminescence of 12% Yb^{3+} -2% Er^{3+} : LaOF

Figure 5.10 (b) Energy level diagram for Upconversion photoluminescence of 12% Yb^{3+} -2% Ho^{3+} : LaOF

Figure 5.10 (c) Energy level diagram for Upconversion photoluminescence of 12% Yb^{3+} -2% Tm^{3+} : LaOF

List of Tables

Table 1.1 Seventeen rare earth elements and their properties

Table 2.1 Structural data of doped La₂O₃ samples extracted from the XRD spectra

Table 2.2 EDAX data of undoped/doped 1% Ln³⁺: La₂O₃ with atomic percentage

Table 2.3 UV-VIS data of the samples

Table 2.4 Structural data of doped La₂O₃ samples extracted from the XRD spectra

Table 3.1 Structural data & lattice parameter of synthesized materials extracted from the XRD spectra

Table 3.2: EDAX data of compounds with weight percentage

Table 3.3 UV / VIS data of Compounds

Table 3.4 Redshift D, Crystal field splitting ε_{cfs} and Centroid shift ε_c of Synthesized Compounds

Table 4.1 Structural data from the XRD spectra of three different synthesis routes

Table 4.2 Structural data of doped La₂O₂S extracted from the XRD spectra

Table 4.3 EDAX data of 1%Ln³⁺: La₂O₂S from the spectrum with Atomic percentage

Table 4.4 UV / VIS data of host La₂O₂S as well as 1%Ln³⁺: La₂O₂S

Table 4.5 Structural data of doped La₂O₂S samples extracted from the XRD spectra

Table 5.1 Structural data of doped LaOF samples extracted from the XRD spectra

Table 5.2 EDAX data of 1% Ln³⁺: LaOF from the spectrum with Atomic percentage

Table 5.3 UV/VIS data of host LaOF as well as 1% Ln³⁺: LaOF

Table 5.4 Structural data of doped La₂O₃ samples extracted from the XRD spectra

Executive Summary

The rapid development of the optical technologies during the past years has notably increased the demand of luminescent materials for a large variety of applications. The advancement in the field of nanotechnology and material science has provided a thrust in exploration of various compounds and materials and has played an important role in optimizing the functionality of the materials. This advancement has worked as a catalyst especially in the area of luminescence which has significantly increased the demand of rare-earth-doped optical materials particularly, owing to their wide range of applicability. The study undertaken here involves the synthesis of Lanthanum Oxysulfide ($\text{La}_2\text{O}_2\text{S}$), Lanthanum Oxide (La_2O_3) and Lanthanum Oxyfluoride (LaOF) and their structural, morphological as well as optical characterizations.

One of the uniqueness of the work lies in employing the furnace combustion technique for the synthesis of Lanthanum Oxysulfide. This approach limits the precursors thereby minimizing the use of resources. The method does not require to pass H_2S , CS_2 or any hazardous gas during the reaction and also consumes less time giving maximum yield.

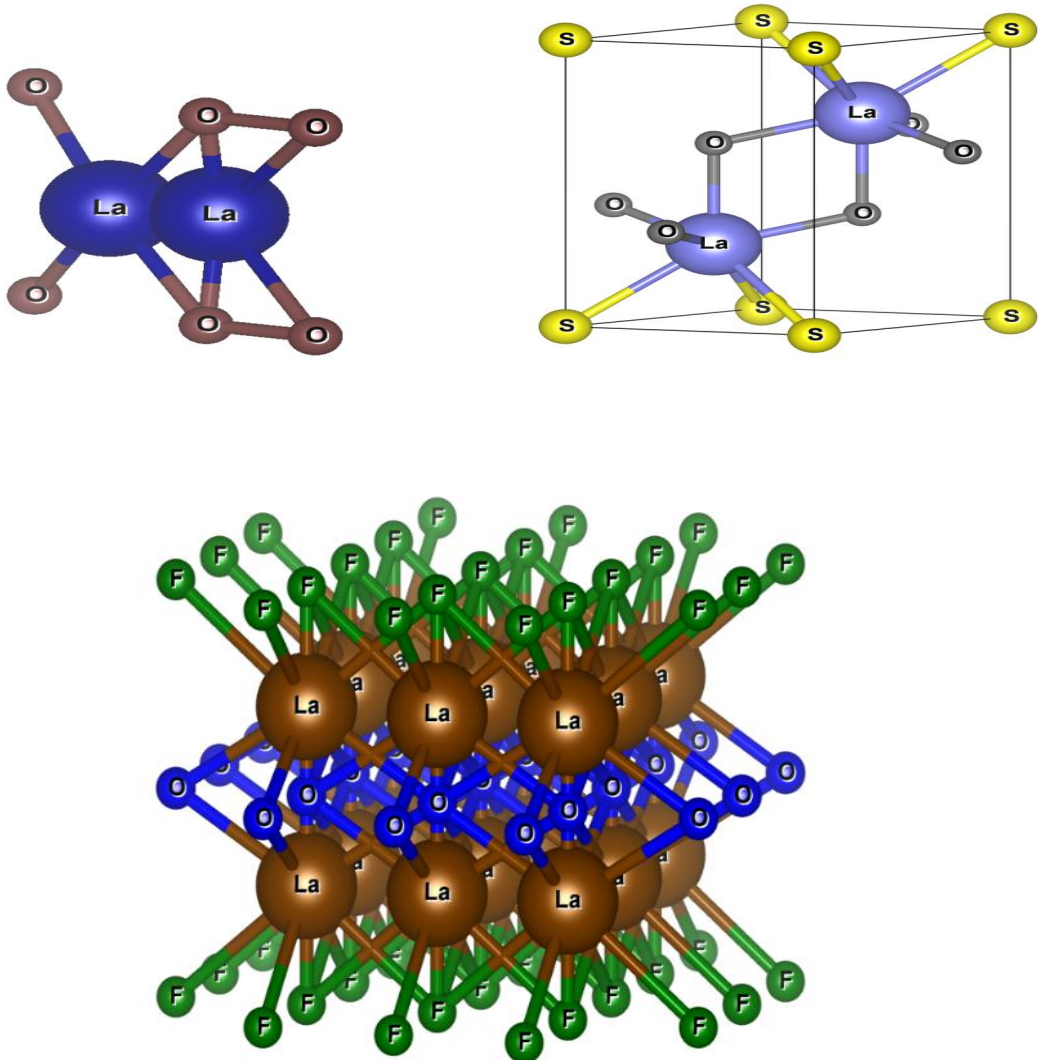
A modified precipitation method has been employed for the synthesis of nanoparticles of La_2O_3 and LaOF . The extract of Aloe Vera leaf called Aloe Vera Gel was used as surfactant for the synthesis of Nanoparticles of La_2O_3 and the extract of Bilva leaf was used as surfactant for the synthesis of Nanoparticles of LaOF .

For the study of down conversion photoluminescence, four different rare earth elements were used as dopant for each of the three compounds. They are Praseodymium, Terbium, Europium, and Dysprosium.

For the study of Upconversion characteristics, six samples of various doping ratio of Ytterbium – Erbium, Ytterbium – Holmium and Ytterbium – Thulium were synthesized for each compound.

Upconversion phosphors are one of the most prospective materials due to their wide application range, the most important being in the bio-medicinal field where they can be used for labeling, sensing, treatment and drug delivery.

The techniques namely XRD, FESEM, EDAX, Particle size analysis, UV-Visible spectroscopy and Photoluminescence spectroscopy were used for structural, morphological, optical studies of the compounds.

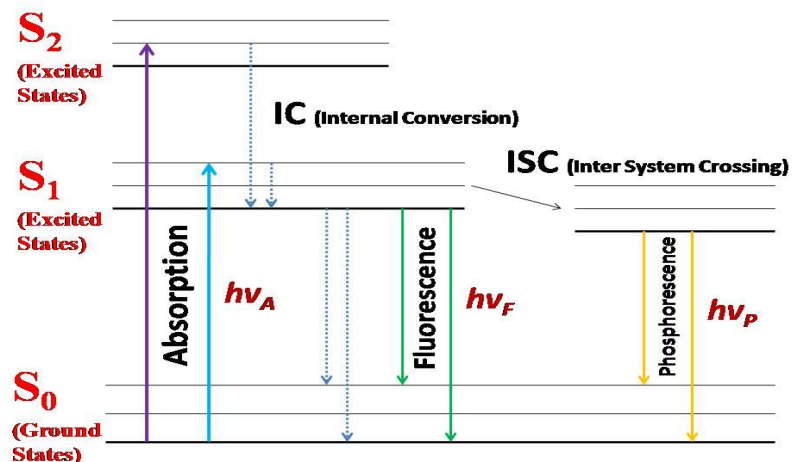


Chapter 1: Luminescence properties of Rare earth elements

Periodic Table of the Elements																					
1	1	H	2													10	2				
2	3	Li	4	Be												He					
3	11	Na	12	Mg												B	C	N	O	F	Ne
4	19	K	20	Ca	Sc	Ti	V	Cr	Mn	Fe	Co	Ni	Cu	Zn	Ga	Ge	As	Se	Br	Kr	
5	37	Rb	56	Sr	Y	Zr	Nb	Mo	Tc	Ru	Rh	Pd	Ag	Cd	In	Sn	Sb	Te	I	Xe	
6	55	Cs	56	Ba	Hf	Ta	W	Re	Os	Ir	Pt	Au	Hg	Tl	Pb	Bi	Po	At	Rn		
7	87	Fr	88	Ra	104	105	106	107	108	109	110	111	112	113	114	115	116	117	118		
LANTHANIDE SERIES		57	58	59	60	61	62	63	64	65	66	67	68	69	70	71					
ACTINIDE SERIES		91	92	93	94	95	96	97	98	99	100	101	102	103	104	105	106	107	108		
Ac	Tm	Pr	Nd	Pm	Sm	Eu	Gd	Tb	Dy	Ho	Er	Tm	Yb	Lu							

[Source:<http://tnahistoryoftechnology.wikispaces.com/Rare+Earth+Metals>]

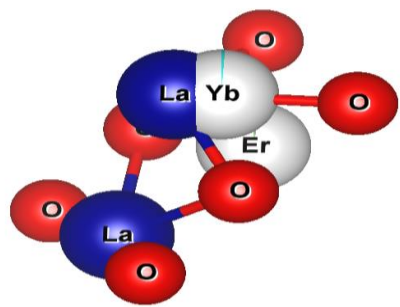
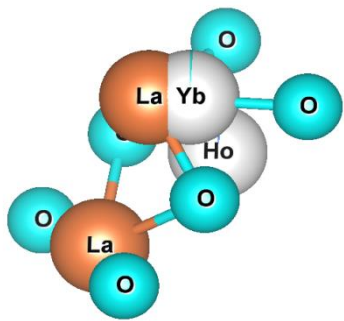
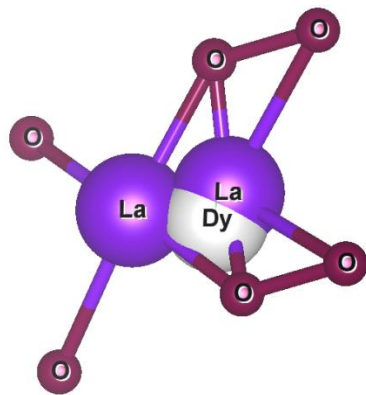
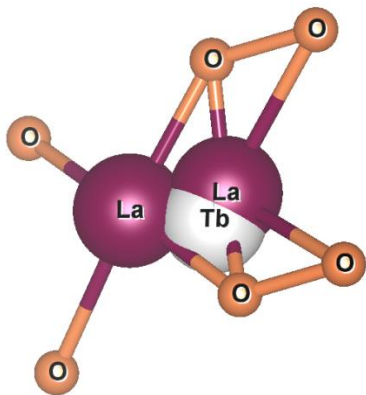
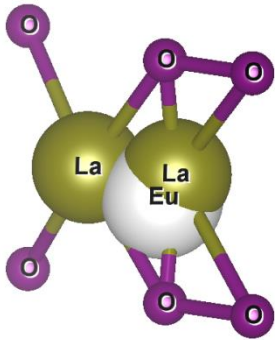
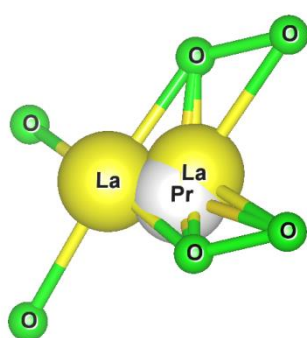
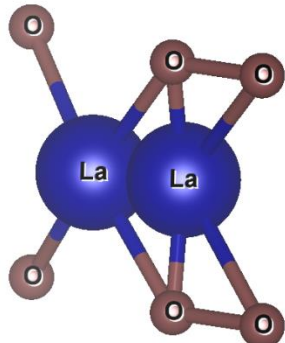
Chapter 1 gives a brief introduction of Luminescence properties of rare earth elements. The chapter starts with the basic introduction of Luminescence, then the mechanism of down conversion photoluminescence and Upconversion Photoluminescence and ends with the discussion on photoluminescence properties of Rare earth elements.

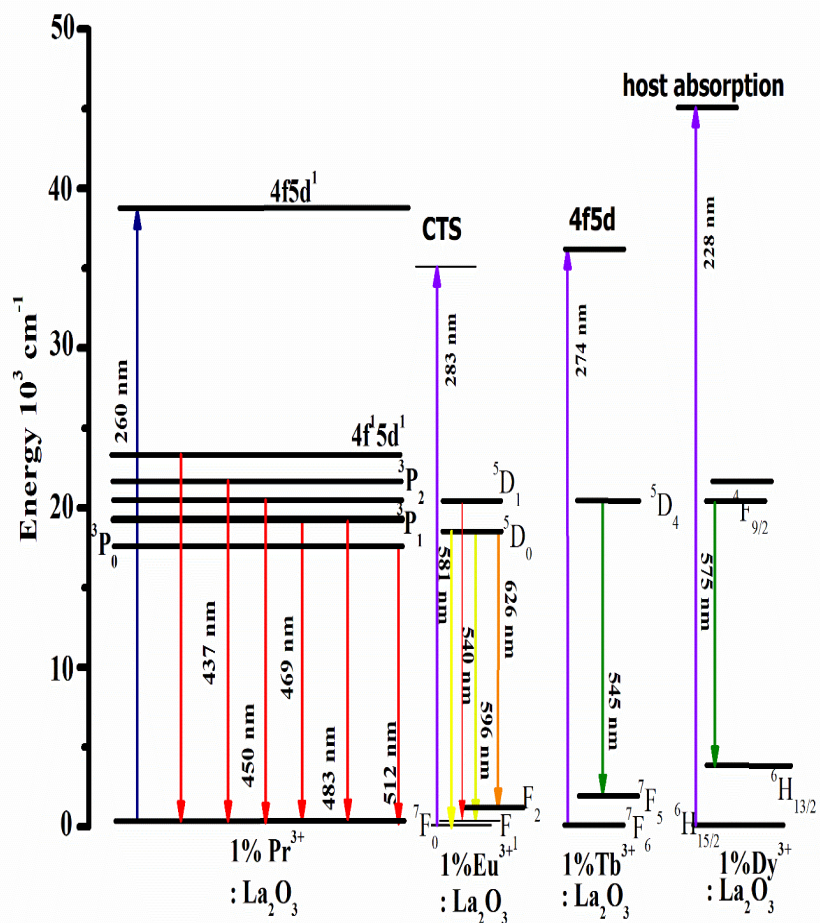
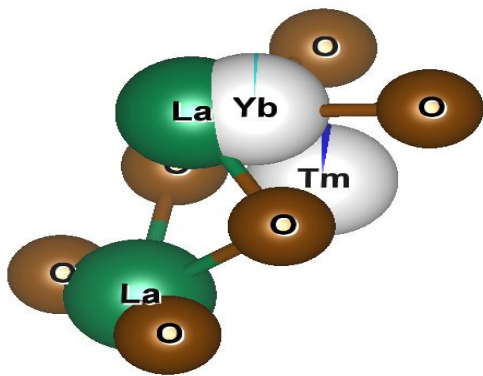


One form of a Jabłński diagram to understand Photoluminescence

Chapter 2: Synthesis & Characterization of Rare Earth Doped La₂O₃:Investigation of Optical, Down conversion and Upconversion Properties

The demand for nanomaterial is increasing day by day due to their wide ranging applications in many areas of science and technology. This has led to a rapid growth of nanotechnology. In this work, a simple route of synthesis for nanoparticles (NP) of La₂O₃ has been attempted. The aloe vera gel assisted precipitation method was used to synthesize NP of undoped as well as doped La₂O₃. Four down conversion compounds 1% Pr³⁺: La₂O₃, 1%Eu³⁺: La₂O₃, 1%Tb³⁺: La₂O₃, & 1%Dy³⁺: La₂O₃ and six upconversion compounds 4% Yb³⁺ - 1% Er³⁺: La₂O₃, 12% Yb³⁺ - 2% Er³⁺: La₂O₃, 4% Yb³⁺ - 1% Ho³⁺: La₂O₃, 12% Yb³⁺ - 2% Ho³⁺: La₂O₃, 4% Yb³⁺ - 1% Tm³⁺: La₂O₃, 12% Yb³⁺ - 2% Tm³⁺: La₂O₃ were also synthesized by this technique. The aloe vera gel acts as a biosurfactant that controls the particle's growth, thus minimizing the particle's size. The structural, elemental, morphological, optical and photoluminescence characterization was carried out on these samples. The XRD & EDAX analysis reveals that the obtained compounds are in the hexagonal phase with high purity having nano crystallite size. The optical bandgap and refractive index have been calculated using the UV – Visible absorption spectra. The average size of synthesized particles was around 60 nm, with a spherical shape, which was confirmed by SEM analysis.



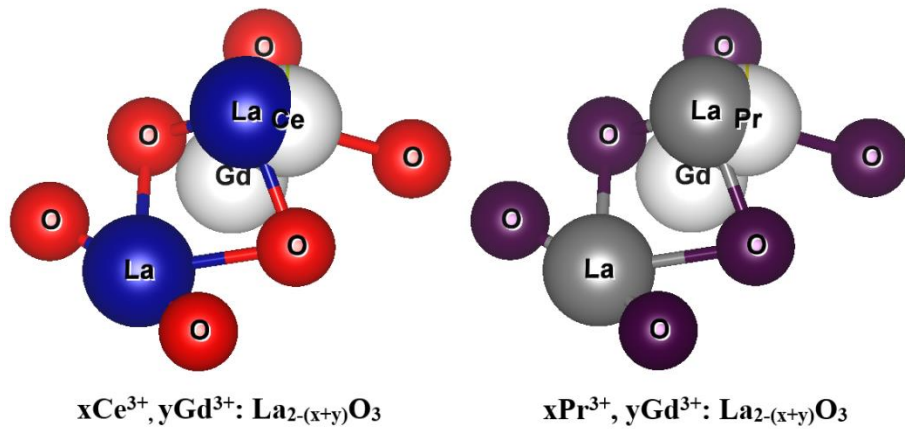
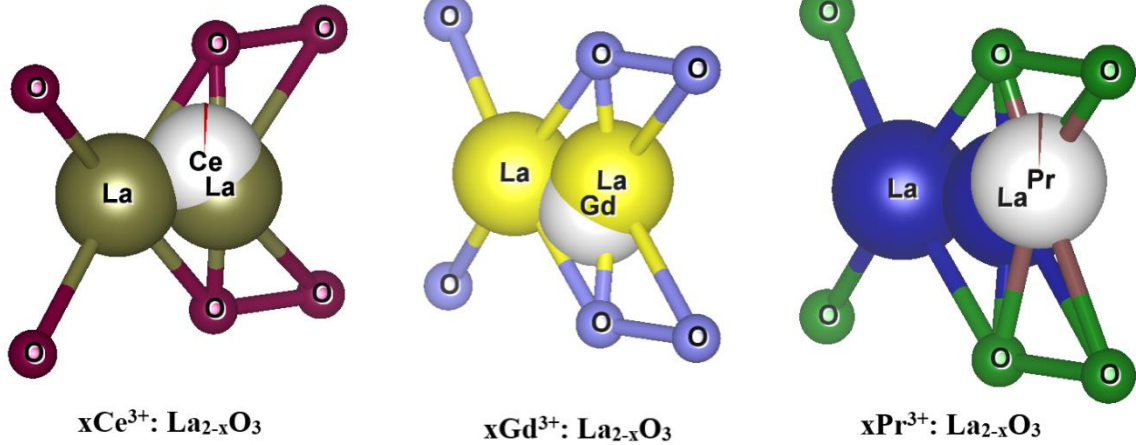


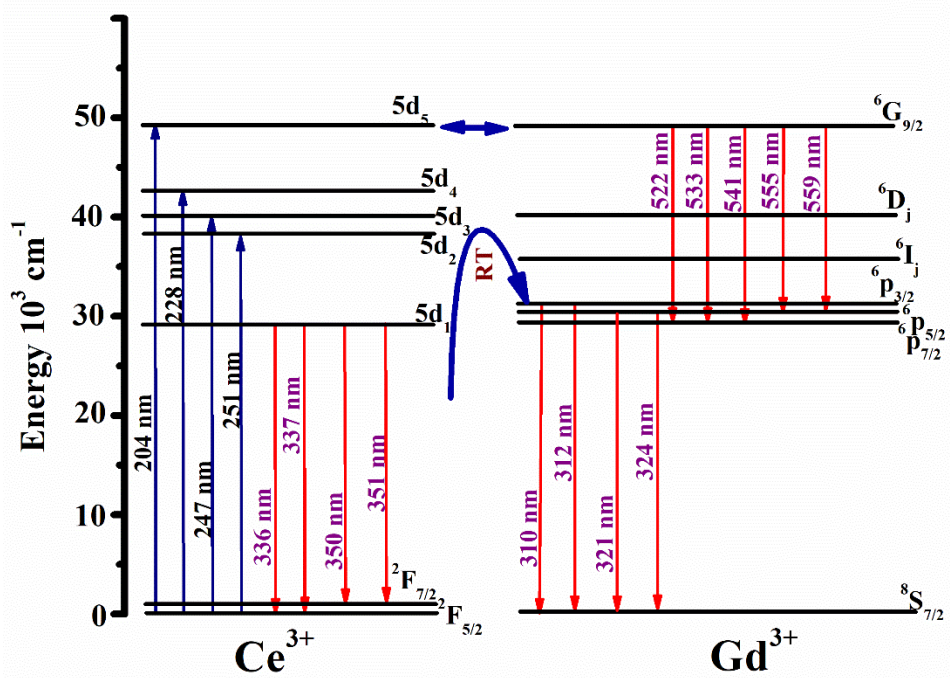
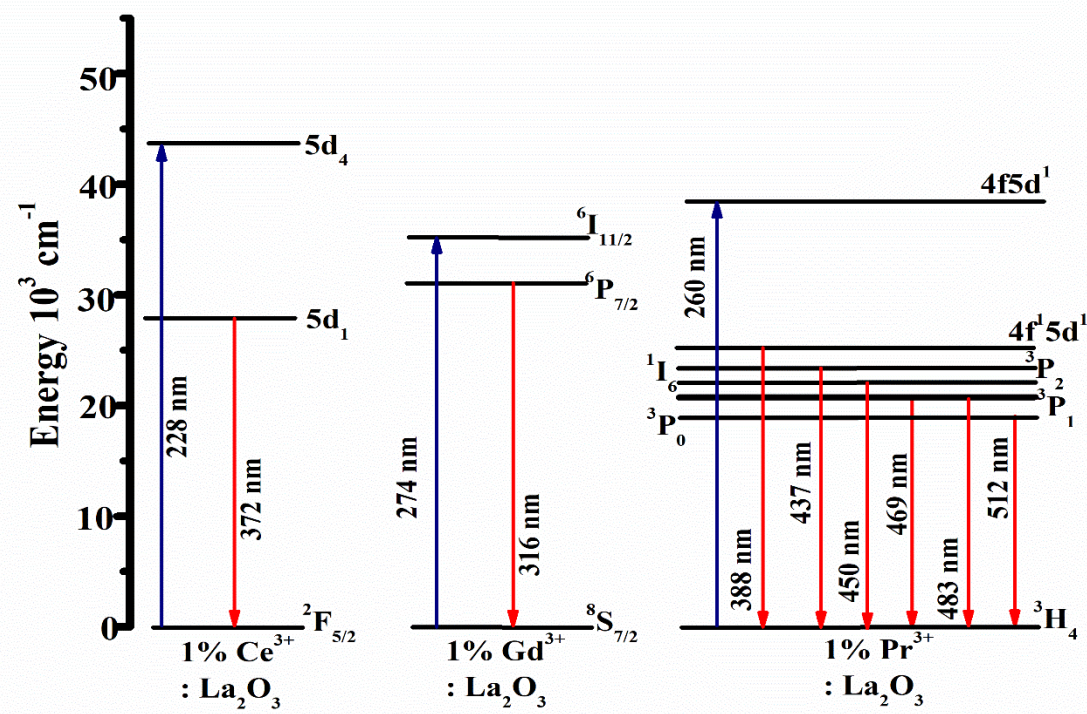
Energy level diagram to understand photoluminescence process

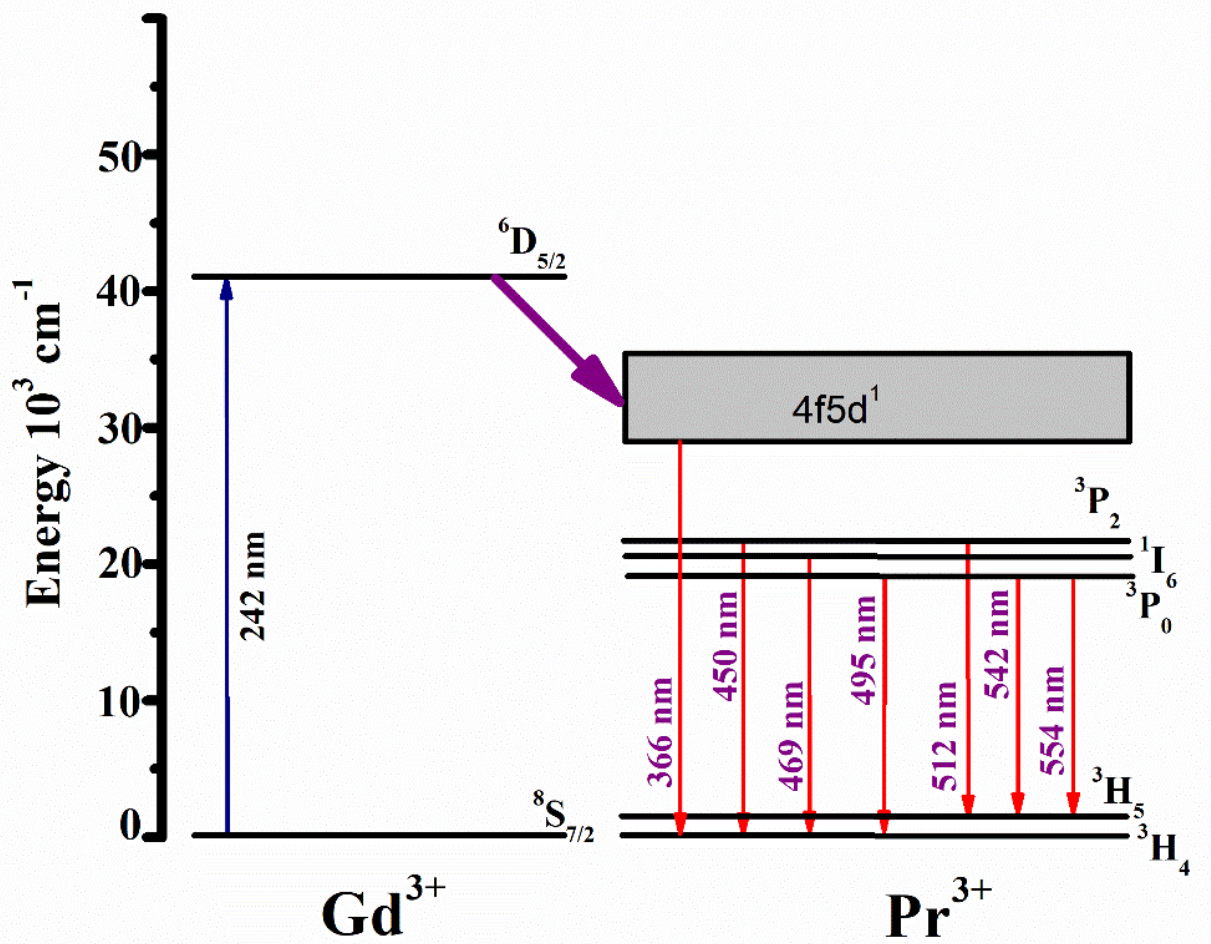
Chapter 3: UV Emission and Energy Transfer Process in $x\text{Ce}^{3+}$,

$y\text{Gd}^{3+} : \text{La}_{2-(x+y)}\text{O}_3$ & $x\text{Pr}^{3+}, y\text{Gd}^{3+} : \text{La}_{2-(x+y)}\text{O}_3$ Phosphors

Despite being a harmful radiation, there are many useful applications of UV radiation. This includes its use in the biomedical field. Hence, it is required to generate the UV radiation with desired characteristics. There are many compounds based on a combination of rare earth elements like Ce, Gd, Pr, which serve as UV emitting phosphors. In this work, seven rare earth based compounds i. e. 1% $\text{Ce}^{3+} : \text{La}_2\text{O}_3$, 1% $\text{Gd}^{3+} : \text{La}_2\text{O}_3$, 1% Ce^{3+} - 1% $\text{Gd}^{3+} : \text{La}_2\text{O}_3$, 2% Ce^{3+} - 1% $\text{Gd}^{3+} : \text{La}_2\text{O}_3$, 1% $\text{Pr}^{3+} : \text{La}_2\text{O}_3$, 1% Pr^{3+} - 1% $\text{Gd}^{3+} : \text{La}_2\text{O}_3$, and 2% Pr^{3+} - 1% $\text{Gd}^{3+} : \text{La}_2\text{O}_3$ have been synthesized to study their UV emission properties and understand the energy transfer process there in. The XRD & EDAX analysis reveals that the obtained compounds possess high purity and are in hexagonal phase with crystallite size in nanometer. The bandgap and refractive index have been calculated from absorption spectra obtained from UV – Visible spectrometer. The emission of 1% $\text{Gd}^{3+} : \text{La}_2\text{O}_3$ falls in UVB region while for 1% $\text{Ce}^{3+} : \text{La}_2\text{O}_3$ & 1% $\text{Pr}^{3+} : \text{La}_2\text{O}_3$, it is in UVA region. Both, UVA and UVB emission has been recorded in 1% Ce^{3+} - 1% $\text{Gd}^{3+} : \text{La}_2\text{O}_3$, 2% Ce^{3+} - 1% $\text{Gd}^{3+} : \text{La}_2\text{O}_3$. In 1% Pr^{3+} - 1% $\text{Gd}^{3+} : \text{La}_2\text{O}_3$ and 2% Pr^{3+} - 1% $\text{Gd}^{3+} : \text{La}_2\text{O}_3$, the emission has been recorded in the visible region with high quantum efficiency due to the energy transfer from Gd^{3+} ion to Pr^{3+} ion and thus has the potential to serve as LED phosphor of cyan color. The parameters like redshift D, centroid shift Σ_c and crystal field splitting Σ_{cfs} have been calculated for Ce & Ce – Gd based La_2O_3 compounds. Compared with previously reported UV emitting phosphors, the compounds synthesized for this work have less complexity in terms of chemical composition and structure. The synthesis process is also relatively simple and eco-friendly with fewer elements used and giving higher yield of products.





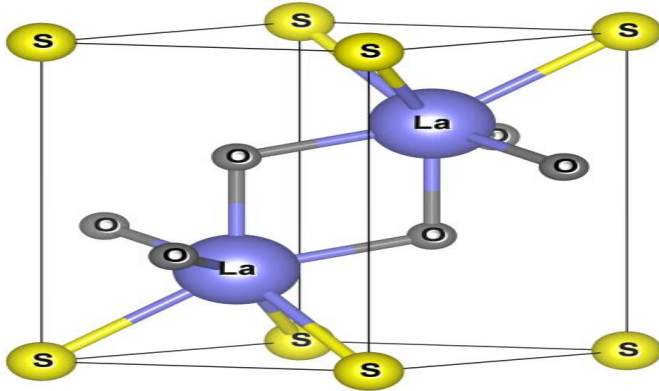


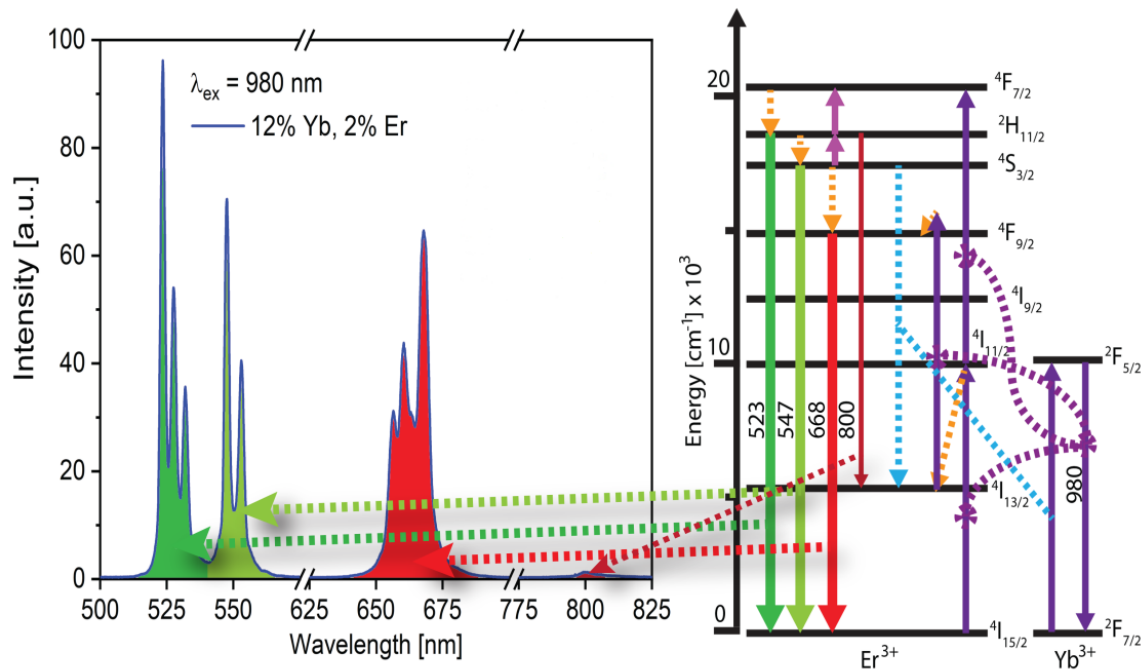
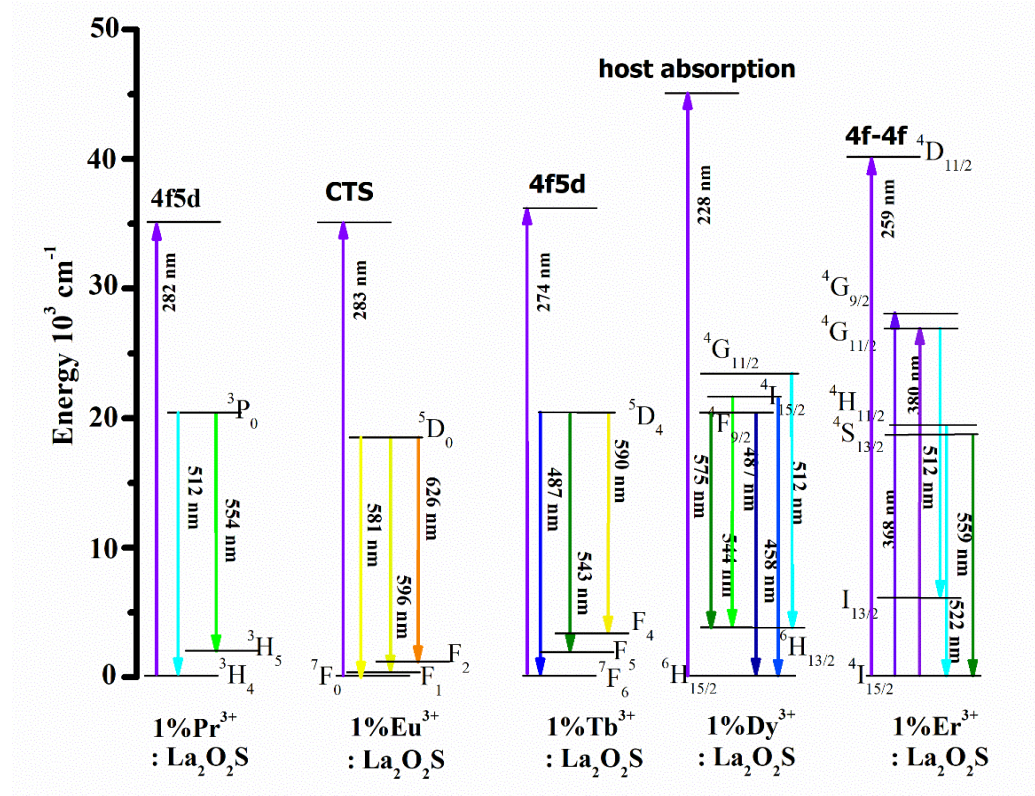
The synthesized compounds have shown emission in UV region and they can be used as UV emitting phosphors. The presence of Gd^{3+} ions alter the energy level of Ce^{3+} ion in Ce^{3+} - Gd^{3+} combination doped La_2O_3 compounds. In the Pr^{3+} - Gd^{3+} combination doped La_2O_3 compound, the emission is predominantly in the visible region with an intense and sharp peak. It has potential to be used as commercial LED phosphor for cyan color.

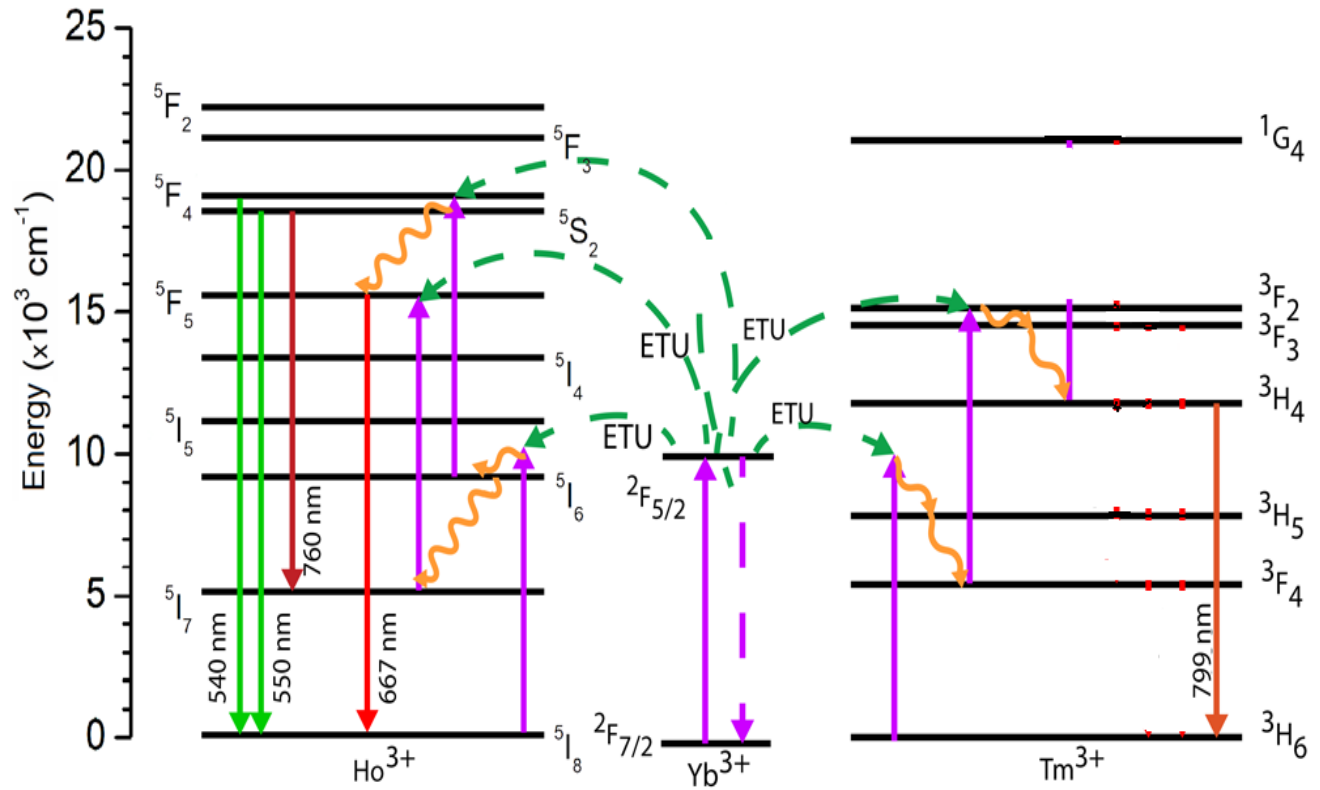
Chapter 4: Synthesis & Characterization of Rare Earth Doped La₂O₂S: Investigation of It's Optical, Down conversion and Upconversion Properties

The Chapter covers two studies. One is a comparative study of structural data from the XRD spectrum of samples synthesized by three different techniques namely, Solid State Technique, Hydrothermal Technique & Furnace Combustion technique for making Lanthanum Oxysulfide Crystal. The comparative study of reveals that the furnace combustion technique without flux is the best technique as the product has perfect hexagonal lattice with space group 164: p $\bar{3}$ m1 and a crystallite size of 31.9 nm. The optical energy band gap of lanthanum oxysulfide synthesized by the furnace combustion technique, calculated from the UV – Visible spectrum is around 4.5 eV. The furnace combustion technique has several advantages that makes it an industrial-friendly approach. It acquired less time for preparation, uses less amount of precursors and doesn't need any pre or post processing. The yield is also high. In the second study, four down conversion samples of 1% Ln³⁺ (Ln = Pr, Eu, Tb, Dy) doped La₂O₂S and six upconversion samples 4% Yb³⁺ - 1% Er³⁺: La₂O₂S, 12% Yb³⁺ - 2% Er³⁺: La₂O₂S, 4% Yb³⁺ - 1% Ho³⁺: La₂O₂S, 12% Yb³⁺ - 2% Ho³⁺: La₂O₂S, 4% Yb³⁺ - 1% Tm³⁺: La₂O₂S, 12% Yb³⁺ - 2% Tm³⁺: La₂O₂S were synthesized by furnace combustion technique. Their structural characteristics as well as optical & photoluminescence properties were investigated. The XRD and EDAX technique was used for structural & elemental analysis. The UV – Visible spectroscopy was used for study of optical properties and the PL spectroscopy was used for photoluminescence studies. The XRD shows that all samples have similar peaks. The peaks match with JCPDS files of hexagonal lattice. EDAX spectra confirmed the incorporation of Ln³⁺ ions in host La₂O₂S. Crystallite size was

found to be in nano meter. UV – Visible studies were used to calculate optical band gap, refractive index, absorption wavelength and molar extinction coefficient. The PL excitation spectra suggest three types of absorption: 4f -5d type absorption in 1% Pr^{3+} : $\text{La}_2\text{O}_2\text{S}$ and 1% Tb^{3+} : $\text{La}_2\text{O}_2\text{S}$; CTS in 1% Eu^{3+} : $\text{La}_2\text{O}_2\text{S}$ and host absorption in 1% Dy^{3+} : $\text{La}_2\text{O}_2\text{S}$. Only three samples, 12% Yb^{3+} -2% Er^{3+} : $\text{La}_2\text{O}_2\text{S}$, 12% Yb^{3+} -2% Ho^{3+} : $\text{La}_2\text{O}_2\text{S}$, 12% Yb^{3+} -2% Tm^{3+} : $\text{La}_2\text{O}_2\text{S}$, among the six gave the upconversion photoluminescence.







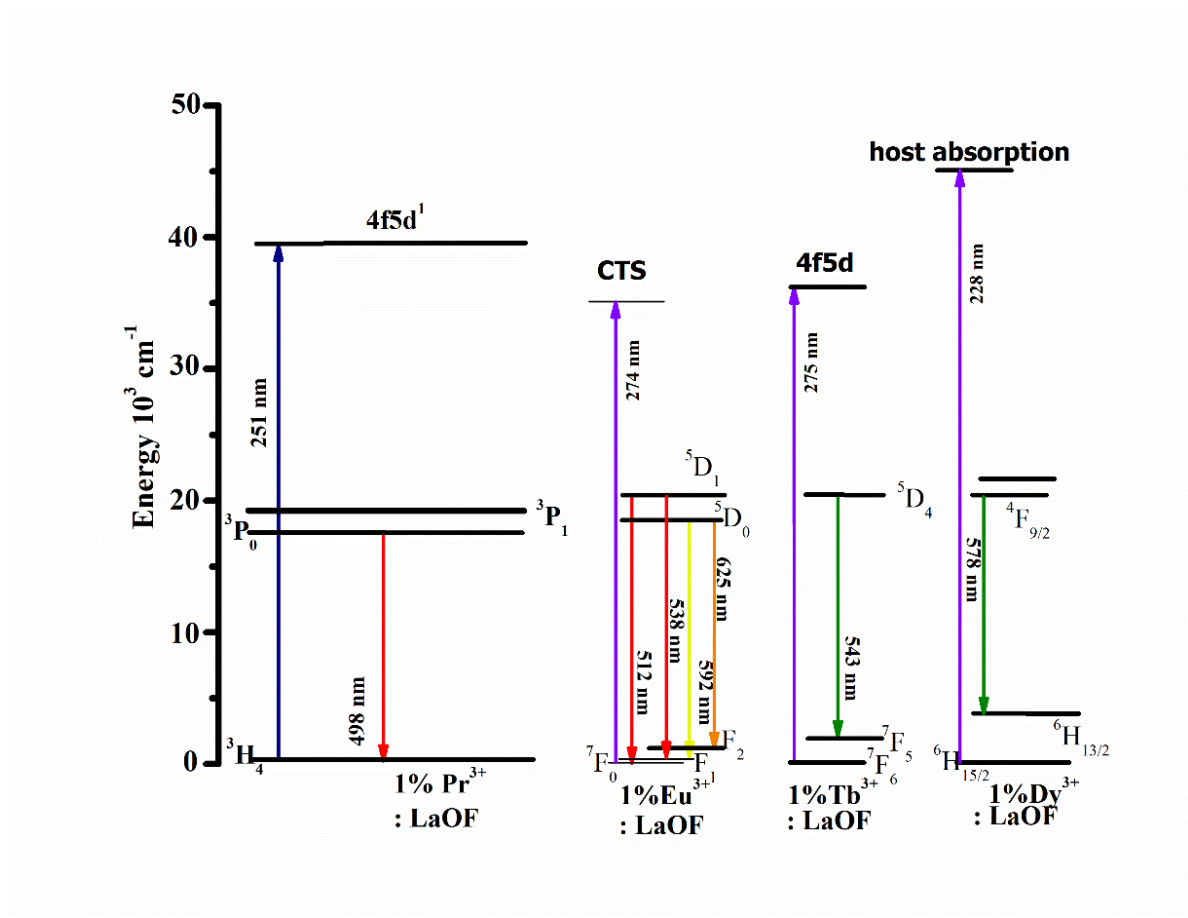
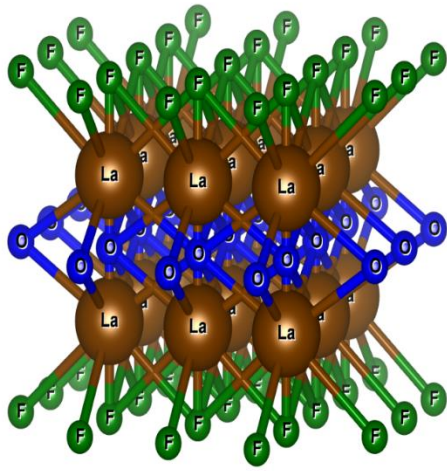
From the comparative study of structural data obtained from the XRD spectra of the three synthesis techniques for the preparation of Lanthanum oxysulfide, the furnace combustion technique without sulfur powder as the flux was found to give the best results. It has the potential to become an industrial friendly technique as it requires less time for synthesis, less number of precursors and gives a perfect hexagonal lattice. Hence, the four down conversion and six upconversion samples were synthesized by using the furnace combustion technique. All peaks were matched with ICDD files that confirmed the perfect hexagonal lattice. The host $\text{La}_2\text{O}_2\text{S}$ had a optical bandgap of 4.96 eV which decreased significantly on doping. The refractive index and molar extinction coefficient were also calculated.

Chapter 5: Synthesis & Characterization of Rare Earth Doped

LaOF:Investigation of Optical, Down conversion and Upconversion

Properties

In this work, a simple route of synthesis for Nanoparticles (NP) of LaOF has been attempted. The Aegle marmelos gel (Bael leaves extract) assisted precipitation method was used to synthesize NP of undoped as well as doped LaOF. Four samples { Pr^{3+} : LaOF, Eu^{3+} : LaOF, Tb^{3+} : LaOF, & Dy^{3+} : LaOF} to study the down conversion properties and six samples {4% Yb^{3+} - 1% Er^{3+} : LaOF, 12% Yb^{3+} - 2% Er^{3+} : LaOF, 4% Yb^{3+} - 1% Ho^{3+} : LaOF, 12% Yb^{3+} - 2% Ho^{3+} : LaOF, 4% Yb^{3+} - 1% Tm^{3+} : LaOF & 12% Yb^{3+} - 2% Tm^{3+} : LaOF} to study the upconversion properties were synthesized by this technique. The Aegle marmelos gel acts as a biosurfactant that controls the particle growth. The structural, elemental, morphological, optical and photoluminescence characterization was carried out on synthesized samples. The XRD & EDAX analysis reveals that the obtained compounds possesses high purity in the hexagonal phase and have crystallite size in nanometer. The optical bandgap and refractive index have been calculated from absorption characteristics obtained from UV – Visible spectra. From the SEM results, the average size of synthesized particles was found to be in the range of 34 nm to 88 nm with spherical shape.



Reference:

- [1] G.H. Dieke, R.A. Satten, Spectra and Energy Levels of Rare Earth Ions in Crystals, Am. J. Phys. (1970). doi:10.1119/1.1976350.
- [2] A.R. Jha, Rare earth materials: Properties and applications, 2014. doi:10.1201/b17045.
- [3] T. Wu, J. Zhou, B. Wu, W. Li, Effect of La₂O₃ content on wear resistance of alumina ceramics, J. Rare Earths. (2016). doi:10.1016/S1002-0721(16)60027-3.
- [4] The rare earth elements: an introduction, Choice Rev. Online. (2016). doi:10.5860/choice.196797.
- [5] W. Wu, F. Zhang, X. Bian, S. Xue, S. Yin, Q. Zheng, Effect of loaded organic phase containing mixtures of silicon and aluminum, single iron on extraction of lanthanum in saponification P507-HCl system, J. Rare Earths. (2013). doi:10.1016/S1002-0721(12)60348-2.
- [6] C.H. Yan, Z.G. Yan, Y.P. Du, J. Shen, C. Zhang, W. Feng, Controlled Synthesis and Properties of Rare Earth Nanomaterials, 2011. doi:10.1016/B978-0-444-53590-0.00004-2.
- [7] Z.G. Yan, C.H. Yan, Controlled synthesis of rare earth nanostructures, J. Mater. Chem. (2008). doi:10.1039/b810586c.
- [8] J. Shen, L.D. Sun, C.H. Yan, Luminescent rare earth nanomaterials for bioprobe applications, Dalt. Trans. (2008). doi:10.1039/b805306e.
- [9] L. Yu, H. Song, S. Lu, Z. Liu, L. Yang, X. Kong, Luminescent properties of LaPO₄:Eu nanoparticles and nanowires, J. Phys. Chem. B. (2004). doi:10.1021/jp047688c.
- [10] G.C. Righini, M. Ferrari, Photoluminescence of rare-earth-doped glasses, Riv. Del Nuovo Cim. (2005). doi:10.1393/ncr/i2006-10010-8.
- [11] C.D.S. Brites, P.P. Lima, N.J.O. Silva, A. Millán, V.S. Amaral, F. Palacio, L.D. Carlos,

Organic-Inorganic Eu³⁺/Tb³⁺ codoped hybrid films for temperature mapping in integrated circuits, *Front. Chem.* (2013). doi:10.3389/fchem.2013.00009.

- [12] A. Kitai, *Luminescent Materials and Applications*, 2008. doi:10.1002/9780470985687.
- [13] L.E. Sobon, K.A. Wickersheim, R.A. Buchanan, R. V. Alves, Growth and properties of lanthanum oxysulfide crystals, *J. Appl. Phys.* (1971). doi:10.1063/1.1660682.
- [14] C.W. Struck, W.H. Fonger, Dissociation of Eu⁺³ charge-transfer state in Y₂O₂S and La₂O₂S into Eu⁺² and a free hole, *Phys. Rev. B.* (1971). doi:10.1103/PhysRevB.4.22.
- [15] R. Vali, Electronic, dynamical, and dielectric properties of lanthanum oxysulfide, *Comput. Mater. Sci.* (2006). doi:10.1016/j.commatsci.2005.08.007.
- [16] C. Koepke, A.J. Wojtowicz, A. Lempicki, Excited-state absorption in excimer-pumped CaWO₄ crystals, *J. Lumin.* (1993). doi:10.1016/0022-2313(93)90003-6.
- [17] C. Li, H. Wang, B. Bai, L. Zhang, Thermodynamic Analysis of Precipitation of La-O-S-As Inclusions in Steel, in: *Miner. Met. Mater. Ser.*, 2019. doi:10.1007/978-3-030-05955-2_75.
- [18] Y. Hou, G. Xiong, L. Liu, G. Li, N. Moelans, M. Guo, Effects of LaAlO₃ and La₂O₂S inclusions on the initialization of localized corrosion of pipeline steels in NaCl solution, *Scr. Mater.* (2020). doi:10.1016/j.scriptamat.2019.10.025.
- [19] B.M. Jaffar, H.C. Swart, H.A.A. Seed Ahmed, A. Yousif, R.E. Kroon, Cathodoluminescence degradation of Bi doped La₂O₃ and La₂O₂S phosphor powders, *Phys. B Condens. Matter.* (2019). doi:10.1016/j.physb.2019.411659.
- [20] L.J.B. Erasmus, H.C. Swart, J.J. Terblans, La₂O₂S:Eu³⁺ stability as temperature sensor, *Appl. Surf. Sci.* (2019). doi:10.1016/j.apsusc.2019.05.075.
- [21] S. Imashuku, K. Wagatsuma, Cathodoluminescence Analysis of Nonmetallic Inclusions in

Steel Deoxidized and Desulfurized by Rare-Earth Metals (La, Ce, Nd), Metall. Mater. Trans. B Process Metall. Mater. Process. Sci. (2020). doi:10.1007/s11663-019-01732-8.

- [22] S. Tan, D. Li, Enhancing Oxygen Storage Capability and Catalytic Activity of Lanthanum Oxysulfide (La₂O₂S) Nanocatalysts by Sodium and Iron/Sodium Doping, ChemCatChem. (2018). doi:10.1002/cctc.201701117.
- [23] Q. Pan, D. Yang, S. Kang, J. Qiu, G. Dong, Regulating Mid-infrared to Visible Fluorescence in Monodispersed Er³⁺-doped La₂O₂S (La₂O₂SO₄) Nanocrystals by Phase Modulation, Sci. Rep. (2016). doi:10.1038/srep37141.
- [24] G. Jiang, X. Wei, Y. Chen, C. Duan, M. Yin, B. Yang, W. Cao, Luminescent La₂O₂S:Eu³⁺ nanoparticles as non-contact optical temperature sensor in physiological temperature range, Mater. Lett. (2015). doi:10.1016/j.matlet.2014.12.057.
- [25] J. Lian, B. Wang, P. Liang, F. Liu, X. Wang, Fabrication and luminescent properties of La₂O₂S:Eu³⁺ translucent ceramic by pressureless reaction sintering, Opt. Mater. (Amst). (2014). doi:10.1016/j.optmat.2014.01.024.
- [26] I. Iparraguirre, J. Azkargorta, O. Merdrignac-Conanec, M. Al-Saleh, C. Chlique, X. Zhang, R. Balda, J. Fernández, Laser action in Nd³⁺-doped lanthanum oxysulfide powders, Opt. Express. (2012). doi:10.1364/oe.20.023690.
- [27] S.V. Yap, R.M. Ranson, W.M. Cranton, D. Koutsogeorgis, Decay time characteristics of La₂O₂S: Eu and La₂O₂S: Tb for use within an optical sensor for human skin temperature measurement, Appl. Opt. (2008). doi:10.1364/AO.47.004895.
- [28] X. xian Luo, W. he Cao, Ethanol-assistant solution combustion method to prepare La₂O₂S:Yb,Pr nanometer phosphor, J. Alloys Compd. (2008). doi:10.1016/j.jallcom.2007.06.011.

- [29] I. Kandarakis, D. Cavouras, Experimental and theoretical assessment of the performance of Gd₂O₂S: Tb and La₂O₂S:Tb phosphors and Gd₂O₂S:Tb-La₂O₂S:Tb mixtures for X-ray imaging, *Eur. Radiol.* (2001). doi:10.1007/s003300000715.
- [30] R.H. Krauss, R.G. Hellier, J.C. McDaniel, Surface temperature imaging below 300 K using La₂O₂S:Eu, *Appl. Opt.* (1994). doi:10.1364/ao.33.003901.
- [31] C. Freiburg, W. Krumpen, U. Troppenz, Determinations of Ce, Eu and Tb in the electroluminescent materials Gd₂O₂S and La₂O₂S by total-reflection X-ray spectrometry, *Spectrochim. Acta Part B At. Spectrosc.* (1993). doi:10.1016/0584-8547(93)80032-P.
- [32] J.A. Bagilo, Lanthanum Oxysulfide as a Catalyst for the Oxidation of CO and COS by SO₂, *Ind. Eng. Chem. Prod. Res. Dev.* (1982). doi:10.1021/i300005a007.
- [33] W.I. Dobrov, R.A. Buchanan, Photoconductivity and luminescence in lanthanum oxysulfide, *Appl. Phys. Lett.* (1972). doi:10.1063/1.1654343.
- [34] Y. Yan, X. Zhang, H. Li, Y. Ma, T. Xie, Z. Qin, S. Liu, W. Sun, E. Lewis, An optical fiber sensor based on La₂O₂S:Eu scintillator for detecting ultraviolet radiation in real-time, *Sensors* (Switzerland). (2018). doi:10.3390/s18113754.
- [35] L. Wang, X. Yang, Q. Zhang, B. Song, C. Wong, Luminescence properties of La₂O₂S:Tb³⁺ phosphors and phosphor-embedded polymethylmethacrylate films, *Mater. Des.* (2017). doi:10.1016/j.matdes.2017.04.003.
- [36] S.W. Kim, T. Hasegawa, T. Abe, H. Nakagawa, S. Hasegawa, K. Seki, K. Toda, K. Uematsu, T. Ishigaki, M. Sato, Abnormal improvement in emission of lanthanum oxysulfide phosphor La₂O₂S:Tb³⁺ synthesized by a novel method, thermal decomposition in eutectic molten salt, *Ceram. Int.* (2016). doi:10.1016/j.ceramint.2016.03.176.

- [37] J. Fernández, R. Balda, M. Barredo-Zuriarrain, O. Merdrignac-Conanec, N. Hakmeh, S. García-Revilla, M.A. Arriandiaga, Spectroscopic and thermal study of Er-doped oxysulfide crystal powders, in: *Laser Refrig. Solids VIII*, 2015. doi:10.1117/12.2076963.
- [38] D. Ma, S. Liu, Y. Zhang, C. Zhang, S. Huang, Controlled synthesis of Eu³⁺-doped La₂O₂S nanophosphors by refluxing method, *J. Exp. Nanosci.* (2013). doi:10.1080/17458080.2011.591002.
- [39] M. Pokhrel, A.K. Gangadharan, D.K. Sardar, High upconversion quantum yield at low pump threshold in Er³⁺/Yb³⁺ doped La₂O₂S phosphor, *Mater. Lett.* (2013). doi:10.1016/j.matlet.2013.02.062.
- [40] L. Yu, F. Li, H. Liu, Fabrication and photoluminescent characteristics of one-dimensional La₂O₂S:Eu³⁺ nanocrystals, *J. Rare Earths.* (2013). doi:10.1016/S1002-0721(12)60285-3.
- [41] E.I. Sal'nikova, D.I. Kaliev, P.O. Andreev, Kinetics of phase formation upon the treatment of La₂(SO₄)₃ and La₂O₂SO₄ in a hydrogen flow, *Russ. J. Phys. Chem. A.* (2011). doi:10.1134/S0036024411120296.
- [42] Z. Liu, X. Sun, S. Xu, J. Lian, X. Li, Z. Xiu, Q. Li, D. Huo, J.G. Li, Tb³⁺- and Eu³⁺-doped lanthanum oxysulfide nanocrystals. Gelatin-templated synthesis and luminescence properties?, *J. Phys. Chem. C.* (2008). doi:10.1021/jp0764687.
- [43] D. Qilin, S. Hongwei, W. Meiyuan, B. Xue, D. Biao, Q. Ruifei, Q. Xuesong, Z. Hui, Size and concentration effects on the photoluminescence of La₂O₂S:Eu³⁺ nanocrystals, *J. Phys. Chem. C.* (2008). doi:10.1021/jp808343f.
- [44] K. Ikeue, T. Kawano, M. Eto, D. Zhang, M. Machida, X-ray structural study on the different redox behavior of La and Pr oxysulfates/oxysulfides, *J. Alloys Compd.* (2008). doi:10.1016/j.jallcom.2007.04.145.

- [45] K. Rajamohan Reddy, K. Annapurna, N. Sooraj Hussain, S. Buddhudu, Fluorescence spectra of Tb^{3+} : $Ln<inf>2</inf>O<inf>2</inf>S$ powder phosphors, Spectrosc. Lett. (1997).
- [46] T. Xia, W.H. Cao, X.X. Luo, Y. Tian, Combustion synthesis and spectra characteristic of Gd_2O_2S : Tb^{3+} and La_2O_2S : Eu^{3+} x-ray phosphors, J. Mater. Res. (2005). doi:10.1557/JMR.2005.0301.
- [47] H. Peng, S. Huang, F. You, J. Chang, S. Lu, Lin Cao, Preparation and surface effect analysis of trivalent europium-doped nanocrystalline La_2O_2S , J. Phys. Chem. B. (2005). doi:10.1021/jp0453414.
- [48] K. Rajamohan Reddy, K. Annapurna, S. Buddhudu, Fluorescence spectra of $Eu^{3+}:Ln_2O_2S$ ($Ln = Y, La, Gd$) powder phosphors, Mater. Res. Bull. (1996). doi:10.1016/0025-5408(96)00129-8.
- [49] J. Ma, M. Fang, N.T. Lau, On the synergism between La_2O_2S and CoS_2 in the reduction of SO_2 to elemental sulfur by CO , J. Catal. (1996). doi:10.1006/jcat.1996.0024.
- [50] S. Buddhudu, F.J. Bryant, Optical transitions of erbium(3+):lanthanum oxide sulfide (La_2O_2S) and erbium(3+):yttrium oxide sulfide (Y_2O_2S), J. Less-Common Met. (1989). doi:10.1016/0022-5088(89)90195-1.
- [51] Y. Kitazawa, Y. Kunimoto, M. Wakihara, M. Taniguchi, Phase equilibria and oxidation mechanisms in the LA-S-O system, J. Therm. Anal. (1982). doi:10.1007/BF01912953.
- [52] K.C. Bleijenberg, F.A. Kellendonk, C.W. Struck, Two-photon excited luminescence of thulium-activated lanthanum oxysulfide ($La_2O_2S-Tm^{3+}$), J. Chem. Phys. (1980). doi:10.1063/1.440583.
- [53] H. Ratinen, X-ray-excited optical fluorescence of ten rare earth ions in Y_2O_2S , La_2O_2S ,

and Gd₂O₂S, Phys. Status Solidi. (1972). doi:10.1002/pssa.2210120211.

- [54] R. Ward, J.J. Pitha, A.L. Smith, The Preparation of Lanthanum Oxysulfide and its Properties as a Base Material for Phosphors Stimulated by Infrared1, J. Am. Chem. Soc. (1947). doi:10.1021/ja01200a009.
- [55] X. Wang, J.G. Li, M.S. Molokeev, Q. Zhu, X. Li, X. Sun, Layered hydroxyl sulfate: Controlled crystallization, structure analysis, and green derivation of multi-color luminescent (La,RE)O₂SO₄ and (La,RE)O₂S phosphors (RE = Pr, Sm, Eu, Tb, and Dy), Chem. Eng. J. (2016). doi:10.1016/j.cej.2016.05.089.
- [56] J. Tauc, R. Grigorovici, A. Vancu, Optical Properties and Electronic Structure of Amorphous Germanium, Phys. Status Solidi. (1966). doi:10.1002/pssb.19660150224.
- [57] V. Kumar, J.K. Singh, Model for calculating the refractive index of different materials, Indian J. Pure Appl. Phys. (2010).
- [58] W.T. Carnall, G.L. Goodman, K. Rajnak, R.S. Rana, A systematic analysis of the spectra of the lanthanides doped into single crystal LaF₃, J. Chem. Phys. (1989). doi:10.1063/1.455853.
- [59] C. Gorller-Walrand, K. Binnemans, Spectral intensities of f-f transitions.pdf, in: Handb. Phys. Chem. Rare Earths Vol 25, 1998.
- [60] Advances in Spectroscopy for Lasers and Sensing, 2006. doi:10.1007/1-4020-4789-4.
- [61] G.H. Dieke, H. Crosswhite, Spectra and Energy Levels of Rare Earth Ions in Crystals, che. 13, Interscience Publishers, 1968.
- [62] I. Ragan, L. Hartson, H. Pidcock, R. Bowen, R. Goodrich, Pathogen reduction of SARS-CoV-2 virus in plasma and whole blood using riboflavin and UV light, PLoS One. 15

(2020) e0233947. doi:10.1371/journal.pone.0233947.

- [63] N. Brownstone, M. Mosca, J. Hong, E. Hadeler, T. Bhutani, Phototherapy for Psoriasis: New Research and Insights, *Curr. Dermatol. Rep.* (2021). doi:10.1007/s13671-020-00324-z.
- [64] H. Stege, K. Ghoreschi, C. Hünefeld, UV phototherapy: UV phototherapy and photodiagnostics—a practical overview, *Hautarzt.* (2021). doi:10.1007/s00105-020-04744-7.
- [65] C.H. Lee, S.B. Wu, C.H. Hong, H.S. Yu, Y.H. Wei, Molecular mechanisms of UV-induced apoptosis and its effects on skin residential cells: The implication in UV-based phototherapy, *Int. J. Mol. Sci.* (2013). doi:10.3390/ijms14036414.
- [66] P. Sahu, V.K. Jain, K. Aggarwal, S. Kaur, S. Dayal, Tacalcitol: a useful adjunct to narrow-band ultraviolet-B phototherapy in vitiligo, *Photodermatol. Photoimmunol. Photomed.* (2016). doi:10.1111/phpp.12265.
- [67] A. Takada, K. Matsushita, S. Horioka, Y. Furuichi, Y. Sumi, Bactericidal effects of 310 nm ultraviolet light-emitting diode irradiation on oral bacteria, *BMC Oral Health.* (2017). doi:10.1186/s12903-017-0382-5.
- [68] R. K.P., F. M.E., A. K.L., F. S.R., A Review of the Use of Tanning Beds as a Dermatological Treatment, *Dermatol. Ther.* (Heidelb). (2015).
- [69] A. Gabet, H. Métivier, C. de Brauer, G. Mailhot, M. Brigante, Hydrogen peroxide and persulfate activation using UVA-UVB radiation: Degradation of estrogenic compounds and application in sewage treatment plant waters, *J. Hazard. Mater.* (2021). doi:10.1016/j.jhazmat.2020.124693.
- [70] A. Nguyen, D. Krupke, M. Burbage, S. Bhatnagar, S.P. Fekete, A.T. Becker, Using a

UAV for Destructive Surveys of Mosquito Population, in: Proc. - IEEE Int. Conf. Robot. Autom., 2018. doi:10.1109/ICRA.2018.8463184.

- [71] C. Zhou, C. Jiang, J. Zhao, P. Zhan, X. Tang, D. Jin, X. Wang, Bi³⁺-doped Ba₂Y_{1-x}Lu_xNbO₆:Bi³⁺ (0 ≤ x ≤ 1.0) solid solution phosphors: tunable photoluminescence and application for white LEDs, Bull. Mater. Sci. (2021). doi:10.1007/s12034-020-02307-z.
- [72] L. Gariazzo, G. Gasparini, A. Casabella, L. Carmisciano, A. Clapasson, F. Murgioni, L. Molfetta, E. Cozzani, A. Parodi, Is ultraviolet radiation avoidance affecting bone health in melanoma patients?, Photodermatol. Photoimmunol. Photomed. (2021). doi:10.1111/phpp.12657.
- [73] H. Luo, L. Zhong, Ultraviolet germicidal irradiation (UVGI) for in-duct airborne bioaerosol disinfection: Review and analysis of design factors, Build. Environ. (2021). doi:10.1016/j.buildenv.2021.107852.
- [74] G.H. Dieke, H.M. Crosswhite, B. Dunn, Emission Spectra of the Doubly and Triply Ionized Rare Earths*, J. Opt. Soc. Am. 51 (1961) 820. doi:10.1364/josa.51.000820.
- [75] X. Qin, X. Liu, W. Huang, M. Bettinelli, X. Liu, Lanthanide-Activated Phosphors Based on 4f-5d Optical Transitions: Theoretical and Experimental Aspects, Chem. Rev. 117 (2017) 4488–4527. doi:10.1021/acs.chemrev.6b00691.
- [76] L. Wu, B. Liu, J. Zhang, B. Han, A novel UV-emitting Ce³⁺ -doped chloroborate Ba₂GaB₄O₉Cl phosphor, Optik (Stuttg.) 184 (2019) 241–246. doi:10.1016/j.ijleo.2019.03.064.
- [77] Z. Zhang, J. Liang, L. Sun, S. Wang, Q. Sun, B. Devakumar, S. Rtimi, X. Huang, Synthesis and photoluminescence properties of near-UV-excitible cyan-emitting

$\text{Ca}_2\text{YHf}_2\text{Ga}_3\text{O}_{12}:\text{Ce}^{3+}$ garnet phosphors, J. Lumin. 227 (2020) 117544. doi:10.1016/j.jlumin.2020.117544.

- [78] P. Dorenbos, T. Shalapska, G. Stryganyuk, A. Gektin, A. Voloshinovskii, Spectroscopy and energy level location of the trivalent lanthanides in $\text{LiY}_2\text{P}_4\text{O}_{12}$, J. Lumin. 131 (2011) 633–639. doi:10.1016/j.jlumin.2010.11.005.
- [79] P. Dorenbos, (formula presented)-level energies of (formula presented) and the crystalline environment. III. Oxides containing ionic complexes, Phys. Rev. B - Condens. Matter Mater. Phys. 64 (2001) 1–12. doi:10.1103/PhysRevB.64.125117.
- [80] I. Milisavljevic, Y. Wu, E. Zych, The effect of Gd^{3+} doping on luminescence properties of (Gd , Ce): SrF_2 nanopowders and transparent ceramics, J. Lumin. 224 (2020) 117243. doi:10.1016/j.jlumin.2020.117243.
- [81] I. Adell, R.M. Solé, M.C. Pujol, M. Lancry, N. Ollier, M. Aguiló, F. Díaz, Single crystal growth, optical absorption and luminescence properties under VUV-UV synchrotron excitation of type III $\text{Ce}^{3+}:\text{KGd}(\text{PO}_3)_4$, a promising scintillator material, Sci. Rep. 8 (2018) 1–11. doi:10.1038/s41598-018-29372-z.
- [82] ENERGY TRANSFER PHENOMENA IN $\text{Li}(\text{Y}, \text{Gd})\text{F}_4$: Ce, Th H.S. KILIAAN*, A. MEIJERINK and G. BLASSE, 35 (1986) 155–161.
- [83] H. Suzuki, T.A. Tombrello, C.L. Melcher, J.S. Schweitzer, Energy transfer from Gd to Ce in $\text{Gd}_2(\text{SiO}_4)\text{O} : \text{Ce}$, J. Lumin. 60–61 (1994) 963–966. doi:10.1016/0022-2313(94)90321-2.
- [84] S.C. Gedam, Optical study of Gd^{3+} and Tb^{3+} in $\text{KZnSO}_4\text{Cl} : \text{Ce}^{3+}$ Phosphor, 1 (2013) 6–10.
- [85] X. Cao, S. Sun, B. Lu, Y. Liu, R. Ma, H. Cao, H. Ma, H. Huang, Spectral

photoluminescence properties of YAG: Ce, R (R: Gd³⁺, Pr³⁺, Gd³⁺ and Pr³⁺) transparent fluorescent thin film prepared by pulse laser deposition, *J. Lumin.* 223 (2020) 117222. doi:10.1016/j.jlumin.2020.117222.

- [86] N. Singh, J.K. Lee, M. Mohapatra, R.M. Kadam, V. Singh, UV emitting Gd incorporated LiBaB₉O₁₅ phosphors: An ESR and photoluminescence investigation, *J. Lumin.* 223 (2020) 117239. doi:10.1016/j.jlumin.2020.117239.
- [87] V. Singh, B.R. Venkateswara Rao, A.S. Rao, J.L. Rao, M. Irfan, Photoluminescence and electron spin resonance study on narrow-band UVB emitting Gd-doped LaPO₄ phosphors, *Optik (Stuttg.)* 206 (2020) 164020. doi:10.1016/j.ijleo.2019.164020.
- [88] D. Shuang, T. Wanjun, X. Guangyong, Y. Yuhong, H. Zhengxi, Synthesis and photoluminescence tuning of (Sr,Ln)9Mg1.5(PO₄)₇ phosphors by Ln (Ln = Y, La, Gd, Lu) substitution, *J. Lumin.* 224 (2020) 1–6. doi:10.1016/j.jlumin.2020.117331.
- [89] R.G. Kunghatkar, P.S. Hemne, S.J. Dhoble, UVB emitting LiSrBO₃phosphor for phototherapy lamp, *AIP Conf. Proc.* 1953 (2018) 3–8. doi:10.1063/1.5032844.
- [90] J.A. Jiménez, Silicon-Induced UV Transparency in Phosphate Glasses and Its Application to the Enhancement of the UV Type B Emission of Gd³⁺, *ACS Appl. Mater. Interfaces.* 9 (2017) 15599–15604. doi:10.1021/acsami.7b03162.
- [91] D.S. Thakare, S.K. Omanwar, P.L. Muthal, S.M. Dhopate, V.K. Kondawar, S. V. Moharil, UV-emitting phosphors: Synthesis, photoluminescence and applications, *Phys. Status Solidi Appl. Res.* 201 (2004) 574–581. doi:10.1002/pssa.200306720.
- [92] Z. Tian, H. Liang, B. Han, Q. Su, Y. Tao, G. Zhang, Y. Fu, Photon cascade emission of Gd³⁺ in Na(Y,Gd)FPO₄, *J. Phys. Chem. C.* 112 (2008) 12524–12529. doi:10.1021/jp802975g.

- [93] Z. Yang, J.H. Lin, M.Z. Su, Y. Tao, W. Wang, Photon cascade luminescence of Gd³⁺ in GdBaB₉O₁₆, *J. Alloys Compd.* 308 (2000) 94–97. doi:10.1016/S0925-8388(00)00908-7.
- [94] B.P. Gangwar, S. Irusta, S. Sharma, Physicochemical and optical properties of one-pot combustion synthesized Pr doped La₂O₃/La(OH)₃, *J. Lumin.* 219 (2020). doi:10.1016/j.jlumin.2019.116893.
- [95] Y. Shimizu, Y. Takano, K. Ueda, UV emissions in Gd³⁺ + doped or Gd³⁺-Pr³⁺ + Co-doped III-III perovskite-type RMO₃ (R = Y, La; M = Al, Ga), *Thin Solid Films.* 559 (2014) 23–26. doi:10.1016/j.tsf.2013.11.135.
- [96] G. Blasse, J.P.M.V.A.N. Vliet, J.W.M. Verwey, R. Hoogendam, M. Wiegel, Blasse G. et al. Luminescence of Pr³⁺ in scandium borate (ScBo₃) and the host lattice dependence of the stokes shift //Journal of Physics and Chemistry of Solids. – 1989. – T. 50. – №. 6. – C. 583-585., 50 (1989) 583–585.
- [97] T. Jiang, B. Du, H. Zhang, D. Yu, L. Sun, G. Zhao, C. Yang, Y. Sun, M. Yu, M.N.R. Ashfold, High-performance photoluminescence-based oxygen sensing with Pr-modified ZnO nanofibers, *Appl. Surf. Sci.* 483 (2019) 922–928. doi:10.1016/j.apsusc.2019.04.053.
- [98] I. Carrasco, K. Bartosiewicz, F. Piccinelli, M. Nikl, M. Bettinelli, Structural effects and 5d→4f emission transition shifts induced by Y co-doping in Pr-doped K₃Lu_{1-x}Y_x(PO₄)₂, *J. Lumin.* 189 (2017) 113–119. doi:10.1016/j.jlumin.2016.08.022.
- [99] J. Ueda, A. Meijerink, P. Dorenbos, A.J.J. Bos, S. Tanabe, Thermal ionization and thermally activated crossover quenching processes for 5d-4f luminescence in Y₃A_{15-x}G_xO₁₂: Pr³⁺, *Phys. Rev. B.* 95 (2017) 1–8. doi:10.1103/PhysRevB.95.014303.
- [100] S. Imashuku, K. Wagatsuma, Cathodoluminescence Analysis of Nonmetallic Inclusions in Steel Deoxidized and Desulfurized by Rare-Earth Metals (La, Ce, Nd), *Metall. Mater.*

Trans. B Process Metall. Mater. Process. Sci. (2020). doi:10.1007/s11663-019-01732-8.

- [101] J. Ma, M. Fang, N.T. Lau, On the synergism between La₂O₂S and CoS₂ in the reduction of SO₂ to elemental sulfur by CO, J. Catal. (1996). doi:10.1006/jcat.1996.0024.
- [102] J. Tauc, R. Grigorovici, A. Vancu, Optical Properties and Electronic Structure of Amorphous Germanium, Phys. Status Solidi. (1966). doi:10.1002/pssb.19660150224.
- [103] V. Kumar, J.K. Singh, Model for calculating the refractive index of different materials, Indian J. Pure Appl. Phys. (2010).
- [104] P. Dorenbos, The 4fn↔4fn-1 5d transitions of the trivalent lanthanides in halogenides and chalcogenides, J. Lumin. 91 (2000) 91–106. doi:10.1016/S0022-2313(00)00197-6.
- [105] S.P. Feofilov, Y. Zhou, H.J. Seo, J.Y. Jeong, D.A. Keszler, R.S. Meltzer, Host sensitization of Gd³⁺ ions in yttrium and scandium borates and phosphates: Application to quantum cutting, Phys. Rev. B - Condens. Matter Mater. Phys. 74 (2006) 1–9. doi:10.1103/PhysRevB.74.085101.
- [106] L. Yu, Y. Han, R. Lin, K. Ge, C. Zhang, J. Zhang, G. Jia, Controllable synthesis and luminescence properties of one-dimensional La₂O₃ and La₂O₃:Ln³⁺ (Ln = Er, Eu, Tb) nanorods with different aspect ratios, J. Lumin. 229 (2021) 117663. doi:10.1016/j.jlumin.2020.117663.
- [107] G. Maheshwaran, R. Selva Muneeswari, A. Nivedhitha Bharathi, M. Krishna Kumar, S. Sudhahar, Eco-friendly synthesis of lanthanum oxide nanoparticles by Eucalyptus globulus leaf extracts for effective biomedical applications, Mater. Lett. 283 (2021) 128799. doi:10.1016/j.matlet.2020.128799.
- [108] M. Xue, M. Wei, H. Sheng, D. Bai, J. Wang, Tunable electronic properties of silicene

based heterojunctions with ultrathin high- κ La₂O₃ gate dielectric, *Superlattices Microstruct.* 147 (2020) 106686. doi:10.1016/j.spmi.2020.106686.

[109] S. Li, Y. Lin, Y. Wu, Y. Wu, X. Li, W. Tian, Ni doping significantly improves dielectric properties of La₂O₃ films, *J. Alloys Compd.* 822 (2020) 2–11. doi:10.1016/j.jallcom.2019.153469.

[110] B. Sharma, A. Thapa, A. Sarkar, Ab-initio study of LD-HfO₂, Al₂O₃, La₂O₃ and h-BN for application as dielectrics in MTJ memory device, *Superlattices Microstruct.* 150 (2021) 106753. doi:10.1016/j.spmi.2020.106753.

[111] N. Wang, X. Zhang, Z. Bai, Fabrication of highly transparent Er³⁺, Yb³⁺:Y₂O₃ ceramics with La₂O₃/ZrO₂ as sintering additives and the near-infrared and upconversion luminescence properties, *J. Alloys Compd.* 842 (2020) 155932. doi:10.1016/j.jallcom.2020.155932.

[112] X. Huang, D. Zhao, L. Ma, C. Deng, L. Li, K. Chen, X. Yang, Effect of La₂O₃ on crystallization of Glass-ceramics, *J. Non. Cryst. Solids.* 536 (2020). doi:10.1016/j.jnoncrysol.2020.120007.

[113] R. Kurtulus, T. Kavas, I. Akkurt, K. Gunoglu, Theoretical and experimental gamma-rays attenuation characteristics of waste soda-lime glass doped with La₂O₃ and Gd₂O₃, *Ceram. Int.* 47 (2021) 8424–8432. doi:10.1016/j.ceramint.2020.11.207.

[114] J. Zhang, Z. Zhang, Y. Jiao, H. Yang, Y. Li, J. Zhang, P. Gao, The graphene/lanthanum oxide nanocomposites as electrode materials of supercapacitors, *J. Power Sources.* 419 (2019) 99–105. doi:10.1016/j.jpowsour.2019.02.059.

- [115] H.C. Swart, R.E. Kroon, Ultraviolet and visible luminescence from bismuth doped materials, *Opt. Mater. X*. 2 (2019) 100025. doi:10.1016/j.omx.2019.100025.
- [116] G. Sharma, A. Kumar, S. Sharma, S.I. Al-Saeedi, G.M. Al-Senani, A. Nafady, T. Ahamad, M. Naushad, F.J. Stadler, Fabrication of oxidized graphite supported La₂O₃/ZrO₂ nanocomposite for the photoremediation of toxic fast green dye, *J. Mol. Liq.* 277 (2019) 738–748. doi:10.1016/j.molliq.2018.12.126.
- [117] L. Yue, F. Chen, K. Yu, Z. Xiao, X. Yu, Z. Wang, B. Xing, Early development of apoplastic barriers and molecular mechanisms in juvenile maize roots in response to La₂O₃ nanoparticles, *Sci. Total Environ.* 653 (2019) 675–683. doi:10.1016/j.scitotenv.2018.10.320.
- [118] P. Liu, Y. Cui, G. Gong, X. Du, J. Wang, X. Gao, M. Jia, J. Yu, Vanadium contamination on the stability of zeolite USY and efficient passivation by La₂O₃ for cracking of residue oil, *Microporous Mesoporous Mater.* 279 (2019) 345–351. doi:10.1016/j.micromeso.2019.01.023.
- [119] B.M. Jaffar, H.C. Swart, H.A.A. Seed Ahmed, A. Yousif, R.E. Kroon, Luminescence properties of Bi doped La₂O₃ powder phosphor, *J. Lumin.* 209 (2019) 217–224. doi:10.1016/j.jlumin.2019.01.044.
- [120] A. Huminic, G. Huminic, C. Fleacă, F. Dumitrache, I. Morjan, Thermo-physical properties of water based lanthanum oxide nanofluid. An experimental study, *J. Mol. Liq.* 287 (2019). doi:10.1016/j.molliq.2019.111013.
- [121] M.U. Azam, M. Tahir, M. Umer, M.M. Jaffar, M.G.M. Nawawi, Engineering approach to enhance photocatalytic water splitting for dynamic H₂ production using La₂O₃/TiO₂

nanocatalyst in a monolith photoreactor, *Appl. Surf. Sci.* 484 (2019) 1089–1101.
doi:10.1016/j.apsusc.2019.04.030.

[122] A. Umar, A.A. Ibrahim, R. Kumar, T. Almas, P. Sandal, M.S. Al-Assiri, M.H. Mahnashi, B.Z. AlFarhan, S. Baskoutas, Fern shaped La₂O₃ nanostructures as potential scaffold for efficient hydroquinone chemical sensing application, *Ceram. Int.* 46 (2020) 5141–5148.
doi:10.1016/j.ceramint.2019.10.258.

[123] G. Cabello-Guzmán, C. Caro-Díaz, A. Fernandez-Perez, G.E. Buono-Core, B. Chornik, Study of the influence of Er/Ln co-doping in La₂O₃ thin films on their up-conversion properties (where Ln = Ho or Nd), *Opt. Mater. (Amst.)* 99 (2020).
doi:10.1016/j.optmat.2019.109579.

[124] N. Jain, R.K. Singh, A. Srivastava, S.K. Mishra, J. Singh, Prominent blue emission through Tb³⁺ doped La₂O₃ nano-phosphors for white LEDs, *Phys. B Condens. Matter.* 538 (2018) 70–73. doi:10.1016/j.physb.2018.03.014.

[125] G. Chen, R. Lei, S. Xu, H. Wang, S. Zhao, F. Huang, Y. Tian, Effect of Li⁺ ion concentration on upconversion emission and temperature sensing behavior of La₂O₃:Er³⁺ phosphors, *J. Rare Earths.* 36 (2018) 119–124. doi:10.1016/j.jre.2017.03.004.

[126] Y. Zhang, W. Li, T. Zhang, B. Yang, Q. Zheng, J. Xu, H. Wang, L. Wang, X. Zhang, B. Wei, The feasibility of using solution-processed aqueous La₂O₃ as effective hole injection layer in organic light-emitting diode, *Solid. State. Electron.* 139 (2018) 54–59.
doi:10.1016/j.sse.2017.10.036.

[127] Z. Sun, G. Liu, Z. Fu, T. Sheng, Y. Wei, Z. Wu, Nanostructured La₂O₃: Yb³⁺/Er³⁺: Temperature sensing, optical heating and bio-imaging application, *Mater. Res. Bull.* 92

(2017) 39–45. doi:10.1016/j.materresbull.2017.04.005.

- [128] A. Siaï, P. Haro-González, K. Horchani-Naifer, M. Férid, La₂O₃: Tm, Yb, Er upconverting nano-oxides for sub-tissue lifetime thermal sensing, Sensors Actuators, B Chem. 234 (2016) 541–548. doi:10.1016/j.snb.2016.05.019.
- [129] P.V.S.S.S.N. Reddy, D. Narendra Babu, G.M.M. Kishore, S. V. Naveen, B. V. Ramana, B. Srinivas, B. V. Naveen, K. Ramachandra Rao, C. Satya Kamal, Polyol derived Bi³⁺ and Er³⁺ co-doped lanthanum oxide nanophosphors for display & LED applications, Mater. Today Proc. 18 (2019) 2118–2122. doi:10.1016/j.matpr.2019.06.485.
- [130] M. Veerasingam, B. Murugesan, S. Mahalingam, Ionic liquid mediated morphologically improved lanthanum oxide nanoparticles by Andrographis paniculata leaves extract and its biomedical applications, J. Rare Earths. 38 (2020) 281–291. doi:10.1016/j.jre.2019.06.006.
- [131] F. V. Molefe, L.L. Noto, M.S. Dhlamini, B.M. Mothudi, V.R. Orante-Barrón, Structural, photoluminescence and thermoluminescence study of novel Li⁺ co-activated lanthanum oxide activated with Dy³⁺ and Eu³⁺ obtained by microwave-assisted solution combustion synthesis, Opt. Mater. (Amst). 88 (2019) 540–550. doi:10.1016/j.optmat.2018.12.025.
- [132] S. Karthikeyan, M. Selvapandian, S. Shanavas, P.M. Anbarasan, R. Acevedo, A role of annealing temperature on the properties of lanthanum oxide (La₂O₃) microplates by reflux routes, Mater. Today Proc. 26 (2019) 3576–3578. doi:10.1016/j.matpr.2019.07.700.
- [133] B.P. Gangwar, S. Irusta, S. Sharma, Physicochemical and optical properties of one-pot combustion synthesized Pr doped La₂O₃/La(OH)₃, J. Lumin. 219 (2020). doi:10.1016/j.jlumin.2019.116893.

- [134] G. Gao, L. Yang, B. Dai, F. Xia, Z. Yang, S. Guo, P. Wang, F. Geng, J. Han, J. Zhu, Investigation of the effect of annealing temperature on optical properties of lanthanum-oxide thin films prepared by sol-gel method, *Surf. Coatings Technol.* 365 (2019) 164–172. doi:10.1016/j.surfcoat.2018.07.001.
- [135] J. Tauc, R. Grigorovici, A. Vancu, Optical Properties and Electronic Structure of Amorphous Germanium, *Phys. Status Solidi.* (1966). doi:10.1002/pssb.19660150224.
- [136] V. Kumar, J.K. Singh, Model for calculating the refractive index of different materials, *Indian J. Pure Appl. Phys.* (2010).
- [137] G.H. Dieke, H.M. Crosswhite, B. Dunn, Emission Spectra of the Doubly and Triply Ionized Rare Earths*, *J. Opt. Soc. Am.* 51 (1961) 820. doi:10.1364/josa.51.000820.

List of Publications:

- 1) Aleksandar Ćirić, Milica Sekulić, **kevil Shah**, B.S. Chakrabarty, Miroslav D. Dramićanin, Upconversion photoluminescence of sub-micron lanthanum oxysulfide particles co-doped with Yb³⁺/Ho³⁺ and Yb³⁺/Tm³⁺ synthesized by optimized combustion technique, **Optical Materials** 120 (2021) 111417, <https://doi.org/10.1016/j.optmat.2021.111417>
- 2) Aleksandar Ćirić, **kevil Shah**, Milica Sekulić, B.S. Chakrabarty, Miroslav D. Dramićanin, La₂O₂S:Er³⁺/Yb³⁺ nanoparticles synthesized by the optimized furnace combustion technique and their high-resolution temperature sensing, **Optik - International Journal for Light and Electron Optics** 245 (2021) 167690, <https://doi.org/10.1016/j.ijleo.2021.167690>

3) **Shah Kevil**, Ćirić, A., Murthy, K.V.R., Chakrabarty, B.S., Investigation of a new way of synthesis for Nano crystallites of $\text{La}_2\text{O}_2\text{S}$ & 1% Ln^{3+} ($\text{Ln} = \text{Pr}, \text{Eu}, \text{Tb}, \text{Dy}, \text{Er}$) doped $\text{La}_2\text{O}_2\text{S}$ and study their structural and optical properties, **Journal of Alloys and Compounds**, 2021, 851, 156725, <https://doi.org/10.1016/j.jallcom.2020.156725>

4) Hirani, D., **Shah Kevil**, Chakrabarty, B.S., Synthesis and optical properties of zirconia (ZrO_2)-polyacrylicacid (PAA) nanocomposites, **International Journal of Scientific and Technology Research**, 2019, 8(12), pp. 4001–4004

5) Kolte, K.R., **Shah Kevil**, Chakrabarty, B.S., Exploring lanthanum sulphide characteristics for its physical properties, **International Journal of Scientific and Technology Research**, 2019, 8(12), pp. 957–961

List of Papers under publication process:

1) **Shah Kevil**, Murthy, K.V.R., Chakrabarty, B.S., **UV emission and energy transfer process in Ce^{3+} , Gd^{3+} , Pr^{3+} and their combination doped La_2O_3 Nano Crystallite Phosphors**
Submitted in **Advanced Optical Materials, Wiley**

2) **Shah Kevil**, Mitesh Ahire, Murthy, K.V.R., Chakrabarty, B.S., **Synthesis of Nanoparticles of La_2O_3 & Ln^{3+} : La_2O_3 phosphors by Aloe Vera Gel assisted precipitation method and study their Photoluminescence properties**
Submitted in **Physical Chemistry Au, ACS**

SEMINARS/CONFERENCES/WORKSHOPS ATTENDED:

- Attend **International Symposium Cum Workshop On Luminescence Materials** on 18-20th December, 2015, Faculty of Technology and Engineering, The M. S. University of Baroda, Vadodara.

- Attend **National Seminar on Recent Scenario in Science and Technology** on 27th February, 2016, Faculty of Technology and Engineering, The M. S. University of Baroda, Vadodara and presented a poster.
- Attend **UGC Sponsored four days “HANDS-ON” workshop on “Industrial Equipments” (HPCL/GC/FTIR/UV – Visible)** on May, 2016, Pramukh Swami Science & H. D. Patel Arts College, Kadi.
- Attend the **International Seminar on Luminescence and Materials** on **16-17th, June, 2017, Nanyang Technological University, Singapore** and presented Oral Presentation.